



HAL
open science

Lost islands in the northern Lesser Antilles: possible milestones in the Cenozoic dispersal of terrestrial organisms between South-America and the Greater Antilles

Jean-Jacques Cornee, Philippe Münch, Mélody Philippon, Marcelle Boudagher-Fadel, Frédéric Quillévéré, Mihaela Melinte-Dobrinescu, Jean-Frédéric Lebrun, Aurélien Gay, Solène Meyer, Lény Montheil, et al.

► To cite this version:

Jean-Jacques Cornee, Philippe Münch, Mélody Philippon, Marcelle Boudagher-Fadel, Frédéric Quillévéré, et al.. Lost islands in the northern Lesser Antilles: possible milestones in the Cenozoic dispersal of terrestrial organisms between South-America and the Greater Antilles. *Earth-Science Reviews*, 2021, 217, pp.103617. 10.1016/j.earscirev.2021.103617 . hal-03191176

HAL Id: hal-03191176

<https://hal.science/hal-03191176v1>

Submitted on 6 Apr 2021

HAL is a multi-disciplinary open access archive for the deposit and dissemination of scientific research documents, whether they are published or not. The documents may come from teaching and research institutions in France or abroad, or from public or private research centers.

L'archive ouverte pluridisciplinaire **HAL**, est destinée au dépôt et à la diffusion de documents scientifiques de niveau recherche, publiés ou non, émanant des établissements d'enseignement et de recherche français ou étrangers, des laboratoires publics ou privés.

1 **Lost islands in the northern Lesser Antilles: possible milestones in the Cenozoic**
2 **dispersal of terrestrial organisms between South-America and the Greater Antilles**
3

4

5 **Jean-Jacques Cornée¹, Philippe Münch², Mélody Philippon¹, Marcelle BouDagher-**
6 **Fadel³, Frédéric Quillévéré⁴, Mihaela Melinte-Dobrinescu⁵, Jean-Frédéric Lebrun¹,**
7 **Aurélien Gay², Solène Meyer^{2, 6}, Lény Montheil², Serge Lallemand², Boris Marcaillou⁶,**
8 **Muriel Laurencin⁷, Lucie Legendre¹, Clément Garroq², Milton Boucard¹, Marie-Odile**
9 **Beslier⁶, Mireille Laigle⁶, Laure Schenini⁶, Pierre-Henri Fabre⁸, Pierre-Olivier Antoine⁸**
10 **Laurent Marivaux⁸ and the GARANTI and ANTITHESIS Scientific Parties.**

11

12 *The GARANTI Scientific Party is composed of:*

13 Agranier, A., Arcay, D., Audemard, F., Beslier, M.O., Boucard, M; Cornée, J.J., Fabre, M.,
14 Gay, A., Graindorge, D., Klingelhofer, A. Heuret, F., Laigle, M., Lallemand, S., Lebrun J.F.,
15 Léticée, J.L., Malengro, D., Marcaillou, B., Mercier de Lepinay, B., Münch, P., Oliot, E.,
16 Oregioni, D., Padron, C., Quillévéré, F., Ratzov, G., Schenini, L. and Yates, B., J.F.

17

18 *The ANTITHESIS Scientific Party is composed of:* Bouquerel, H., Conin, M., Crozon, J., Dellong,
19 D., De Min, L., de Voogd, B., Evain, M., Fabre, M., Graindorge, D., Gwandai, W., Heuret,
20 A., Klingelhofer, F., Laigle, M., Lallemand, S., Laurencin, M., Lebrun, J.-F., Legendre, L.,
21 Lucazeau, F., Mahamat, H., Marcaillou, B., Mazabraud, Y., Pichot, T., Prunier, C., Renouard,
22 A., Rolandonne, F., Rousset, D., Schenini, L., Thomas, Y., Vitard C.

23

24 ¹ *Géosciences Montpellier, CNRS-Université des Antilles-Université de Montpellier, F-97159*

25 *Pointe à Pitre, Guadeloupe, France*

26 ² *Géosciences Montpellier, CNRS-Université de Montpellier-Université des Antilles, F-34095*

27 *Montpellier, France*

28 ³ *Office of the Vice-Provost (Research), University College London, 2 Taviton Street, London*

29 *WC1H 0BT, UK*

30 ⁴ *Université Claude Bernard Lyon 1, ENS de Lyon, CNRS, UMR 5276 LGL-TPE, F-69622*

31 *Villeurbanne, France*

32 ⁵ *National Institute of Marine Geology and Geoecology, 23–25 Dimitrie Onciul Street, PO*
33 *Box 34–51, 70318 Bucharest, Romania*

34 ⁶ *Geoazur, Université de la Côte d’Azur, CNRS, Observatoire de la Côte d’Azur, IRD, F-*
35 *06560 Valbonne, France*

36 ⁷ *Laboratoire d’Océanologie et Géosciences, Université de Lille, 59655 Villeneuve d’Ascq,*
37 *France*

38 ⁸ *Institut des Sciences de l’Evolution de Montpellier (ISE-M), Univ Montpellier, CNRS, IRD,*
39 *EPHE, F-34095 Montpellier, France*

40
41 Corresponding author: Jean-Jacques Cornée, jean-jacques.cornee@gm.univ-montp2.fr

42 Université des Antilles, Dépt. Géologie, Campus de Fouillole, F-97159 Pointe à Pitre Cedex,
43 Guadeloupe, FWI

44

45 **Keywords: Lesser Antilles, Cenozoic basins, biostratigraphy, seismic stratigraphy,**
46 **palaeogeography, vertical motions**

47

48 **ABSTRACT**

49 Our study aims to reconstruct the palaeogeography of the northern part of the Lesser Antilles in
50 order to analyse whether emerged areas might have existed during the Cenozoic, favouring
51 terrestrial faunal dispersals between South America and the Greater Antilles along the present-day
52 Lesser Antilles arc. The stratigraphy and depositional environments of the islands of Anguilla, St
53 Martin, Tintamarre, St Barthélemy, Barbuda and Antigua are reviewed in association with
54 multichannel reflection seismic data acquired offshore since the 80's in the Saba, Anguilla and
55 Antigua Banks and in the Kalinago Basin, including the most recent academic and industrial surveys.
56 Seven seismic megasequences and seven regional unconformities are defined, and calibrated from
57 deep wells on the Saba Bank and various dredges performed during marine cruises since the 70's in
58 the vicinity of the islands. Onshore and offshore correlations allow us to depict an updated and
59 detailed sedimentary organisation of the northern part of the Lesser Antilles from the late Eocene to
60 the late Pleistocene. Paleogeographic reconstructions reveal sequences of uplift and emergence
61 across hundredwide areas during the late Eocene, the late Oligocene, the early middle-Miocene and
62 the latest Miocene-earliest Pliocene, interspersed by drowning episodes. The ~200 km-long and ~20
63 km-wide Kalinago Basin opened as an intra-arc basin during the late Eocene - early Oligocene. These
64 periods of emergence may have favoured the existence of episodic mega-islands and transient

65 terrestrial connections between the Greater Antilles, the Lesser Antilles and the northern part of the
66 Aves Ridge (Saba Bank). During the Pleistocene, archipelagos and mega-islands formed repeatedly
67 during glacial maximum episodes.

68

69 **1. INTRODUCTION**

70

71 The Caribbean, including the Greater and Lesser Antilles located at the northeastern edge
72 of the Caribbean Plate, are regarded as one of the most important centres of insular
73 biodiversity (Myers al., 2000; Mittermeier et al., 2011). Despite decades of studies, the
74 phylogenetic origins and historical biogeography of this astonishing biodiversity remain,
75 however, controversial (e.g., Hedges et al., 1992; MacPhee and Iturralde-Vinent, 1995, 2005;
76 Iturralde-Vinent and MacPhee, 1999; Myers et al., 2000; Hedges, 2001, 2006; Ali, 2012). In
77 an island setting, either over-water transports (natural rafts of matted vegetation) or land
78 connections provide possible routes for dispersal of terrestrial organisms and their
79 colonization of these remote Caribbean islands. If over-water dispersals by rafting are
80 sweepstake dispersals (and as such hardly predictable), the possibility of over-land (via land-
81 bridges) dispersals relies on the regional tectono-magmatic evolution of the Lesser Antilles
82 subduction zone.

83 Biogeographic models for Antillean terrestrial organisms derive from limited
84 palaeontological and phylogenetic inferences (either based on the morphology or on
85 genes/proteins of living and recently extinct species) (Hedges, 1996; Woods et al., 2001;
86 Graham, 2003; Roca et al., 2004; MacPhee, 2005; Fabre et al., 2014; Brace et al., 2015, 2016;
87 Courcelle et al., 2019; Delsuc et al., 2019; Presslee et al., 2019; Marivaux et al., 2020). They
88 also derive from still controversial paleogeographic models of the Caribbean Plate evolution
89 (e.g., Stephan et al., 1990; Iturralde-Vinent and MacPhee, 1999; Pindell and Kennan, 2009)
90 and global reconstructions (Blakey, <https://deeptimemaps.com/>; Scotese; 2016). The main

91 discussed model for explaining the arrival of many terrestrial organisms of South American
92 origin on the Caribbean islands relate to a possible 2 Myrs- long period of subaerial exposure
93 of the Aves Ridge (Fig. 1) at the Eocene-Oligocene transition. Following this model, the ridge
94 momentarily constituted a land-bridge (named GAARlandia, for land of **G**reater **A**ntilles–
95 **A**ves **R**idge) between northern South America and the Greater Antilles (e.g., MacPhee and
96 Iturralde-Vinent, 1995; Iturralde-Vinent and MacPhee, 1999; MacPhee, 2005; Iturralde-
97 Vinent, 2006)).

98 Contrary to the Aves Ridge, the potential contribution of the Lesser Antilles in early
99 dispersals of South American faunas and flora has never been considered. This is paradoxical
100 because the archipelago is located closer to the subduction deformation front and has
101 experienced uplift and drowning events likely favouring land-organism dispersals and
102 subsequent insular evolution. This is particularly obvious in the Guadeloupe archipelago
103 where repeated uplifts, leading to subaerial exposures, and subsequent drownings have been
104 evidenced (Cornée et al., 2012; Münch et al., 2013, 2014; De Min et al., 2014). Further north,
105 it has been proposed that the Pleistocene rodent *Amblyrhiza*, an endemic giant chinchilloid
106 caviomorph from Anguilla, St Martin and St Barthélemy islands, could be closely related to
107 early Oligocene chinchilloids from Puerto Rico (Velez-Juarbe et al., 2014; Marivaux et al.,
108 2020), thereby extending the evolutionary history of this rodent group back to 30 Ma, and
109 revealing its widespread distribution between the Greater Antilles and the northern Lesser
110 Antilles through time.

111 In this work, we study the palaeogeographic evolution of the northeastern part of the
112 Lesser Antilles during the Cenozoic, as it may have constituted an episodic emerged area
113 between the Aves Ridge to the southwest and the Greater Antilles to the North: the GrANoLA
114 land -Greater Antilles- Northern Lesser Antilles land (Philippon et al., 2020a). Previous
115 bathymetric reconstructions and offshore-onshore geological investigations have suggested

116 that the Kalinago intra-arc rift basin (Figs. 1, 2) may have undergone substantial vertical
117 motion (e.g., Bouysse et al., 1985a; Mann et al., 1995; Feuillet et al., 2011) and 15%
118 extension (Legendre et al., 2018). In the whole Eastern Caribbean (Aves Ridge, Greater and
119 Lesser Antilles), accurate constraints on the chronology, duration and spatial extent of land
120 emergence and drowning during the Cenozoic are, however, strongly missing to reconstruct
121 the regional paleogeographic evolution. This lack of information prevents the effective testing
122 of biogeographic models deriving from gene-based and morpho-anatomical phylogenies and
123 associated divergence time estimates. In this work, we refine the sedimentology and
124 stratigraphy of the deposits over an area extending from the Saba Bank to the Antigua Bank
125 encompassing the Kalinago Basin (Figs. 1, 2), and use these analyses to reconstruct the
126 vertical motions that occurred in this key area of the Northern Lesser Antilles. The study is
127 based on new onshore palaeoenvironmental, biostratigraphic, and structural data, combined
128 and correlated with new offshore-dredged samples and seismostratigraphic interpretation of
129 seismic reflection data from the ANTITHESIS (Marcaillou and Klingelhoefer, 2013; 2016)
130 and GARANTI cruises (Lebrun and Lallemand, 2017), which allow us to reconstruct the
131 palaeogeographic evolution of the region.

132

133 **2. TECTONO-MAGMATIC EVOLUTION OF THE NE CARIBBEAN SINCE** 134 **THE CRETACEOUS**

135

136 The westward subduction of the Proto-Caribbean/Atlantic Ocean lithosphere beneath the
137 Caribbean Plate initiated from Cuba southward during the Cretaceous. The Great Arc of the
138 Caribbean (GAC) is the magmatic expression of this subduction. Magmatic arc samples from
139 the southern Aves Ridge and Leeward Antilles offshore Venezuela indicate that subduction
140 occurred there since the middle-late Cretaceous (Coniacian; Neill et al., 2011) or after

141 Santonian (Hastie et al., 2021). During the Paleocene and the early Eocene, the motion of the
142 North American Plate relative to the Caribbean plate changed from north-eastward to
143 eastward (Pindell and Kennan, 2009; Boschman et al., 2014). At the same time, the collision
144 of the Bahamas Bank margin with the Caribbean Plate sutured the subduction along its
145 northern part (accreting Cuba to the North American plate) whereas a new E-W trending
146 transform plate boundary formed along the proto-Cayman Trough that started opening (e.g.,
147 Pindell and Kennan, 2009; Boschman et al., 2014). Subsequently, the Greater Antilles
148 underwent sinistral shearing and were dismembered along the new transform plate boundary
149 (Fig. 1). The present-day trench curvature of the northern Lesser Antilles subduction zone and
150 along strike variation of the convergence obliquity most likely results from this Eocene
151 reorganisation of the plate boundary and subsequent left lateral motion of the Bahamas Bank /
152 Cuba margin relative to the Caribbean Plate interior (Boschman et al., 2014; Philippon and
153 Corti, 2016; Philippon et al., 2020b). Today, the Greater and Lesser Antilles margins are
154 separated by an elongated, fault-bounded basin, the Anegada Trough (e.g., Jany et al., 1990;
155 Laurencin et al., 2017 and references therein; Fig. 1). Based on dredged samples and seismic
156 reflection profiles, the opening of the Anegada Trough is supposed to have occurred during
157 the middle or the late Miocene (Jany et al., 1990), and its activity has probably been
158 negligible since 2 Ma (Chaytor and ten Brink, 2015; Calais et al., 2016). Our study area lies
159 south of this major tectonic structure separating the Greater from the Lesser Antilles (Fig. 1).

160 Three phases of arc magmatism are recognized along the Antillean subduction zone, with
161 lateral variation with time:

162 (i) arc magmatism was first established during the Late Cretaceous-Paleocene along the
163 Aves Ridge (Fig. 1) as part of the GAC (ages of arc magmatic rocks range between 88 Ma
164 and 59 Ma; Fox et al., 1971; Bouysse et al., 1985a; Neill et al., 2011).

165 (ii) The GAC then migrated eastward (*i.e.*, trenchward) probably during the middle
166 Eocene, as evidenced by the occurrence of Lutetian lavas in the Grenadines Islands
167 (Westercamp et al., 1985). This Eocene arc is present beneath the southern Lesser Antilles
168 islands, and, from Martinique northward, Eocene to earliest Miocene remnants of this arc are
169 exposed and dated in the forearc domain (Westercamp, 1988; Bouysse and Westercamp,
170 1990; Legendre et al., 2018) (Fig. 1). Along the northern Lesser Antilles, this arc is exposed
171 and dated based on radiometric data in Antigua (middle Eocene to earliest Miocene; Nagle et
172 al., 1976; Briden et al., 1979; Mascle and Westercamp, 1983; Weiss, 1994), St Barthélemy
173 (middle Eocene to latest Oligocene; Legendre et al., 2018), and St Martin (late Eocene to
174 early Oligocene; Nagle et al., 1976; Briden et al., 1979). Late Paleogene volcanoclastic arc (or
175 backarc) rocks have also been found in deformed zones of the Virgins Islands, Puerto-Rico
176 and Anguilla (Briden et al., 1979; Andréieff et al., 1988; Jolly et al., 1998; Rankin, 2002),
177 thereby suggesting that the remnant arc extended across the incipient Anegada Trough at this
178 time. These rocks, nevertheless, have never been related neither to those of the Aves Ridge
179 nor to those of the Grenada Basin.

180 (iii) The modern arc (inner arc of Mc Cann and Sykes, 1984) is formed 50 km west of the late
181 Paleogene-early Neogene remnant one (outer arc of Mc Cann and Sykes, 1984). From
182 Guadeloupe northward, volcanism occurred since the early Pliocene (e.g., Samper et al.,
183 2007; Favier et al., 2019; Carey et al., 2020). The northernmost island of the arc is Saba
184 where volcanism occurred during the Late Pleistocene (Defant et al., 2001). Offshore north of
185 Saba, Pliocene volcanic and volcanoclastic rocks have been dredged from the Luymes Bank
186 (cruise ARCANTE 1) and the Noroît Seamount (cruise ARCANTE 3, 118) (Figs. 1 and 2)
187 (Bouysse et al., 1981; 1985b).

188

189 **3. GEOLOGICAL SETTING OF THE NE CARIBBEAN ISLANDS**

190

191 ***3.1. Anguilla Bank***

192 Three main islands emerge from the large, shallow water Anguilla Bank: from north to
193 south Anguilla, St Martin (including the islet of Tintamarre) and St Barthélemy (Fig. 2).
194 Neogene deposits are exposed on these three islands (Christman 1953; Andréieff et al., 1987;
195 1988; older references therein).

196 St Martin consists of 2000 to 3000 m-thick Eocene volcanoclastic turbidites intruded
197 by late Eocene-early Oligocene granodiorites (28.4-31.3 Ma; Nagle et al., 1976; Briden et al.,
198 1979). In the southwestern part of the island, late Oligocene magmatic rocks may also occur
199 but remain undated (Andréieff et al., 1988, 1989). On the southwestern and eastern margins of
200 the island, Neogene carbonates deposited unconformably on Paleogene rocks, which were
201 tilted along a NE-SW fault bounding the northwestern coast of the island. Drilled cores from
202 the southwestern deposits recovered up-to-250 m of Neogene carbonates along the margin of
203 the island (Terres Basses; Dagain et al., 1989). On the islet of Tintamarre, the basal part of the
204 Neogene deposits remains unknown. According to Andréieff et al. (1988), the deposits at St
205 Martin and Tintamarre constitute two main formations with unknown relationships: 1) > 70
206 m- thick sedimentary rocks which were deposited during the late Burdigalian in a reefal
207 depositional setting; 2) 80 m- thick distal forereef sedimentary rocks which were deposited
208 between the late Serravallian and the Messinian in St Martin only.

209 In the island of Anguilla, the oldest sedimentary deposits consist of late Paleocene to
210 Eocene volcanoclastic turbidites tilted to the south-east (Andréieff et al., 1988). These
211 turbidites are unconformably overlaid by a 100 m- thick biostromal coral reef deposit
212 considered to be either early Miocene or middle Miocene (Andréieff et al., 1988; Budd et al.,
213 2005). Shallow water carbonates are poorly known from other islets of the Anguilla Bank,

214 Sombrero (Pliocene) and Dog Islands (late Burdigalian-early Langhian; Bouysse et al., 1985a;
215 Andréieff et al., 1987).

216 During the cruises ARCANTE, dredged samples have been collected on flanks of the
217 Anguilla Bank (Bouysse and Guennoc, 1983; Bouysse et al., 1985a) (Fig. 2). On the
218 southwestern margin of the Anguilla Bank, dredges 46V and 47V yielded Pleistocene to
219 Holocene carbonate sediments. On the northern margin, dredge 121D provided Pliocene-?
220 Pleistocene tuff limestones, Serravallian marls, and late Eocene magmatic rocks (36.5 to 33
221 Ma interval, whole rock K-Ar ages; Bouysse et al., 1985a). Finally, to the east of the Bank,
222 dredges E402 and ST31 yielded uppermost Cretaceous radiolarian-bearing limestones and
223 Pleistocene clays, respectively.

224

225 **3.2. *Kalinago Basin***

226 The Kalinago Basin is a NW-SE trending, 100 km- long intra-arc rift separating the
227 Anguilla Bank from the recent active volcanic arc (Bouysse et al., 1985a; Jany et al., 1990)
228 (Fig. 2). The basin is bounded by syn- to post- Neogene faults and possibly comprise
229 deformed, Cretaceous to Oligocene or Miocene rocks overlain by poorly deformed, 2.000 m-
230 thick Neogene to Pleistocene deposits (Jany, 1989; Jany et al., 1990; Church and Allison,
231 2004). At the northern margin of the basin on slopes of the Aguillita Spur, dredge RV-
232 Eastward 1390 (Fig. 2) yielded clays and marls that were deposited between the Pliocene and
233 the Pleistocene (Jany, 1989). In the southern part of the basin, southeast of Montserrat (Fig.
234 2), the Integrated Ocean Drilling Program (IODP) Leg 340 (out of Fig. 2) drilled 181 m of
235 late Pleistocene volcanoclastic deposits (Coussens et al., 2012).

236

237 **3.3. *Saba Bank***

238 The shallow water Saba Bank (Figs. 1 and 2) has been intensively explored for oil
239 prospecting (Warner, 1990; Larue and Warner, 1991; Daly, 1995; Church and Allison, 2004;
240 Matchette-Downes, 2007). On the basis of seismic investigations and wells SBD1 (total depth
241 of 2977 m; Marathon Group) and SBD2 (total depth of 4231 m; Fina Group), the bank
242 comprises from bottom to top: 1) a deformed Cretaceous to Paleocene sedimentary basement
243 topped by an unconformity; 2) a subaerial, at least 120 m- thick, porphyritic andesitic
244 sequence dated at 34.4 ± 3.7 Ma and 37.3 ± 1.4 Ma (whole rock K-Ar); 3) a *ca* 900 to 1000
245 m- thick “turbidite” unit dated from the early late Eocene to the early Oligocene based on
246 planktonic foraminifera and calcareous nannofossils; this unit correlates with late Eocene
247 reefs developed on palaeostructural highs; 4) a *ca* 1500 m- thick volcanoclastic “fluvio-
248 deltaic” unit, which were deposited between the early late Oligocene and the early Miocene
249 based on calcareous nannofossils and benthic foraminifera, and 5) an “upper carbonate unit”,
250 which was deposited between the middle Miocene and the early Pliocene based on planktonic
251 foraminifera, and which indicates a shallowing-upward trend (Church and Allison, 2004).

252 North of the Saba Bank, a Pliocene (*ca* 4 Ma) volcanic activity has been evidenced on
253 the Luymes Bank and the Noroît Seamount and may correspond to the northeastern
254 termination of the active volcanic Lesser Antilles Arc (Bouysse et al., 1985a; b). Along with
255 volcanic rocks and clasts, Pliocene-Pleistocene pelagic limestones were mainly recovered and
256 coral reefs and red-algal limestones were also dredged. Finally, one dredge (119D) south of
257 the Noroît Seamount yielded some porphyritic andesite fragments dated at 66.5 ± 1.5 Ma
258 (whole rock K-Ar; Bouysse et al., 1985a), corresponding, like in the Saba Bank and St Croix
259 Island, to the Maastrichtian-Danian GAC basement (Speed et al., 1979) (Fig. 2).

260

261 **3.4. Antigua Bank**

262 The Antigua island comprises three main lithostratigraphic units with an estimated
263 total thickness of 2.500 m. These units are tilted northeastward on the footwall of the normal
264 faults forming the NE side of the Kalinago Basin (e.g., Martin Kayes, 1969; Frost and Weiss,
265 1979; Mascle and Westercamp, 1983; Multer et al., 1986; Weiss, 1994; Donovan et al., 2014;
266 Robinson et al., 2017): 1) the Basal Volcanic Complex (1500 m- thick), poorly constrained as
267 either middle Eocene or Oligocene (39.7-23 Ma; *in* Briden et al., 1979); 2) the Central Plain
268 Group (500 m- thick), composed of volcanoclastic deposits with freshwater and marine
269 limestones, supposed to have been deposited during the Oligocene (Mascle and Westercamp,
270 1983; Robinson et al., 2017); 3) the late Oligocene Antigua Formation, composed of shallow
271 water limestones evolving eastward into deep marine limestones.

272 The Barbuda island consists of four shallow water carbonate formations (Fm.)
273 separated by subaerial erosional surfaces (Brasier and Mather, 1975), from bottom to top: the
274 Highland Fm. (bank edge facies, 40 m- thick at least), Beazer Fm. (fringing reefs, 5 m- thick;
275 Pleistocene), Codrington Fm. (fringing and barrier reefs, 5 m- thick; late Pleistocene) and
276 Palmetto Fm. (eolian dunes, reef, lagoon, and beach deposits, 10 m- thick; Holocene). The
277 age of the Highland Fm. is still debated: Oligocene (Reed, 1921), middle Miocene (Brasier
278 and Mather, 1975), early Pliocene (Brasier and Donahue, 1985; Watters et al., 1991) or
279 Pleistocene (Russell and Mc Intire, 1966; Land et al., 1967; Martin Kaye, 1969).

280 Four dredges performed during the ARCANTE cruises provided reliable information
281 (Andréieff et al, 1980; Bouysse and Guennoc, 1983) (Fig. 2). On the western margin of the
282 Antigua Bank (also eastern margin of the Kalinago rift), dredge 71D yielded Pliocene to
283 Pleistocene bioclastic limestones from an outer reef depositional setting. On the eastern side
284 of the bank, dredge 79D, collected between 1,800 and 2,000 m depths, yielded late Oligocene
285 carbonates from outer-ramp setting and early Miocene pelagic micritic limestones. Above, at

286 480 m depth, dredge 80D yielded late Miocene marls and Pliocene pelagic carbonate deposits.
287 On top the of the bank, at 30 m depth, dredge 78V yielded recent reefal limestones.

288

289 **4. METHODS AND DATA**

290

291 ***4.1. Rock-samples analyses***

292 New field investigations were conducted in 2015, 2017 and 2020 onshore in Anguilla,
293 St Martin and Tintamarre islands with respectively 7, 7 and 6 logged and sampled sections
294 (Appendices C, D, E). For biostratigraphic analyses, 18 samples were collected in Anguilla,
295 17 in St Martin and 24 in Tintamarre. Combined with field-investigations and
296 sedimentological information, the biostratigraphic analyses allow a correlation between the
297 sections and provide a revised lithostratigraphic sketch of the onshore Neogene deposits of the
298 Anguilla Bank. This onshore sampling was completed by seven offshore carbonate samples
299 collected from three rock-dredge hauls carried out during the GARANTI cruise (Fig. 2):
300 Dredge DR GA-04-01 was collected on the northern steepest flank of the Martinita Seamount;
301 Dredge DR GA-04-02 was collected on the southern flank of this Martinita Seamount
302 ; and Dredge GA-03-01 was collected on the Southeastern Spur (Appendix I). For the island
303 of St Barthélemy, we use the recently published results of Cornée et al. (2020) (Appendix G).
304 In Barbuda, we logged and sampled the Highland Fm. (Appendix F) in 2006; 19 samples were
305 collected. In Antigua, 10 samples were chosen for thin sections in order to refine the age of
306 the Antigua Fm. (Appendix G).

307 Across the whole studied area, a total of 125 polished thin sections were obtained from
308 each carbonate rock-type sample in order to analyse their microfacies and fossil content. The
309 identified microfacies were attributed to a depositional environment following the
310 classification of Wright and Burchette (1996), supplemented by the larger benthic

311 foraminiferal content (BouDagher-Fadel, 2008) (e.g., Appendix B). In addition, 18 soft rock
312 samples were washed over a 65 μm screen and the residues were analysed for foraminiferal
313 biostratigraphy. Finally, standard smear-slides were also prepared for 14 of these soft rock
314 samples for calcareous nannofossil analyses (Appendix A). Our biostratigraphical analyses
315 are based on a complete inventory of larger benthic foraminifera, planktonic foraminifera and
316 calcareous nannofossil taxa found in the thin sections and standard smear-slides. We used the
317 zonal schemes and bio-events calibrations of BouDagher-Fadel (2013, 2015, 2018) for
318 planktonic and larger benthic foraminifera, and those of Backman et al. (2012) for calcareous
319 nannofossils, which have been calibrated against the time scale of Gradstein et al. (2012).

320 Finally, we used the $\text{Ar}^{40}/\text{Ar}^{39}$ method to date a large boulder (50 cm) of a fresh
321 porphyritic andesite reworked in submarine lahar deposits overlain by Neogene limestones in
322 the southwestern part of St Martin Island (details are given in Appendix K).

323

324 *4.2. Seismic reflection profiles*

325 We analyzed eight new profiles from the GARANTI cruise that occurred in 2017 on
326 board *L'Atalante* R/V (Lebrun and Lallemand, 2017), together with a set of multichannel
327 reflection seismic lines recorded during cruises ANTITHESIS 1 (2013) and 3 (2017)
328 (Marcaillou and Klingelhoefer, 2013; 2016) (Fig. 2). Acquisition parameters for the selected
329 MCS lines include a 3.902 inches^3 airgun array source and a 720 channels-6.25m trace spacing
330 streamer ensuring a 120-fold coverage. Quality control and binning of the MCS data were
331 performed on board using QCSispeed® and SolidQC® (Ifremer), and processing was
332 performed using GEOVATION® (CGG). Processing sequence includes band-pass (2–7–60–
333 80 Hz) and FK filtering, Spherical divergence and amplitude (gain) correction, predictive
334 deconvolution, three steps velocity analysis and Normal Move-Out (NMO) correction,
335 external mutes, internal mutes and further multiple attenuation by 2D-Surface-Related

336 Multiple Elimination and Radon domain filtering, velocity stack and constant velocity
337 (1500m/s) FK migration.

338 Our data set also includes petroleum seismic data acquired in 2D in the 80's over the
339 Saba Bank and an industrial database on the Saba Bank (Fina 1980; Aladdin 1988). These
340 seismic data, described in Church and Allison (2004), show a lower resolution as compared to
341 those of the GARANTI and ANTITHESIS lines. They allow us, however, to extend our
342 interpretation to a zone that is nowadays closed to seismic investigations. We also benefited
343 from other seismic lines from the "Comité d'Etude Pétrolière et Marine" (CEPM) under the
344 supervision of the "Institut Français du Pétrole et des Énergies Nouvelles" (IFPEN) acquired
345 in the 70's during the Antilles IV cruise (e.g., Bouysse et al., 1985a; b; Bouysse and Mascle,
346 1994). The seismic stratigraphy of the Saba Bank petroleum surveys was calibrated by using
347 two exploration wells (SBD1 and SBD2; Church and Allison, 2004). The CPEM lines in the
348 vicinity of the Antigua Bank were calibrated using offshore-onshore correlations (Legendre,
349 2018), wells IODP 340 (Coussens et al., 2012) and dredges ARCANTE 1 (Andréieff et al.,
350 1980).

351 Seismic facies and units are determined following the classical criteria of Mitchum and
352 Vail (1977) and Roksandic (1978).

353

354 **5. RESULTS**

355

356 **5.1. Onshore**

357 *5.1.1. Anguilla*

358 Seven sections of Anguilla (Appendix C) yielded stratigraphically significant taxa of
359 larger benthic foraminifera (Appendix B) and calcareous nannofossils (Appendix A). Based
360 on the identified taxa, we were able to date each of the logged and sampled sections (Fig. 3).

361 Above Paleogene turbiditic beds tilted to the SE (Crocus Bay section; Andréieff et al., 1988)
362 (Fig. 4A), we found 60 m- thick coral boundstones organized into coral banks and low-relief
363 domes where platy and massive colonies dominate (Fig. 4, B, C, E, F). Associated with the
364 boundstones, we found some bioclastic packstones with abundant corals, larger benthic
365 foraminifera (miogypsinids, amphisteginids, miliolids, and soritids, e.g., *Archaias*), echinoids,
366 red algae, mollusks (pectinids and oysters), and frequent *Teredo* in life position (Fig. 4D). Ten
367 genera and eighteen species of hermatypic corals occur in this platform, among which the
368 *Porites* genus is dominant, the next most abundant being *Montastraea* and *Stylophora* (Budd
369 et al., 1995). Our biostratigraphic analyses indicate that the succession encompasses the
370 Aquitanian to Tortonian-Messinian interval (N4-N18, 23-5.33 Ma) and, except the local
371 occurrence of hardgrounds, no clear evidence of hiatuses has been found in the field. Beds are
372 vertically stacked but low-angle cross-bedded units were found prograding southeastward
373 along the southern coast (e.g., localities ANG3, 9 and 10) and in the northeastern part of the
374 island (ANG 6) (Appendix C).

375 The Neogene deposits of Anguilla likely correspond to those of an isolated shallow
376 reefal, protected inner platform (Fig. 3), as already suggested by Budd et al. (2005) based on
377 the study of some coral build-ups. This platform contains units with prograding beds towards
378 the SE, indicating that it was opening towards a deeper marine setting.

379

380 5.1.2. *St Martin*

381 Above tilted Paleogene volcanoclastic rocks, the succession of the southwestern part of
382 the island comprises, from bottom to top (Fig. 5; localities in Appendix D):

383 1. **10 to 18 m- thick coral reef boundstones and associated bioclastic packstones**
384 (Fig. 6A to C). In the Sabannah area, 4 m- high patch reefs with branching colonies are
385 exposed. Larger benthic foraminifera are mainly represented by miogypsinids and

386 amphisteginids. Planktonic foraminifera (globigerinids) and calcareous nannofossils are also
387 present. At Mullet Bay, we found cross-bedded packstones with red algae and foraminifera
388 and some coral beds. The benthic foraminiferal assemblages are dominated by amphisteginids
389 and *Asterigerina*. Elsewhere, in the Juliana Bay and Kool Hill sections, well bedded bioclastic
390 limestones and coral banks are exposed. Foraminifera are dominated by *Archaias*,
391 *Praerhapydionina*, *Cyclorbiculina*, *Miosorites*, *Androsinopsis* and *Miarchaias*, associated
392 with small miliolids and textulariids. At Kool Hill, karstic cavities infilled by red silty clays
393 and associated with a paleosol level indicate a temporary emersion (Fig. 7C). Our
394 biostratigraphical analyses indicate that the lower part of these deposits correlates with
395 planktonic foraminiferal Zone N5 (latest Aquitanian-early Burdigalian, 21-18 Ma) and the
396 upper part with Zones N6-N8a (late Burdigalian, ~18-15.97 Ma) (Appendix D). The late
397 Burdigalian deposits of the Juliana Airport road section (Fig. 7A) are affected by
398 synsedimentary normal faults (Fig. 7A, B) associated with a local subaerial erosion surface
399 with karstic gullies. Karstic microcaves were found only below this surface, which confirms
400 the existence of a temporary emersion (Fig. 7C-E).

401 **2. 31 m- thick bioturbated wackestone with intercalations of packstone and**
402 **breccias.** The wackestones yielded planktonic and benthic foraminifera as well as red algae.
403 The packstones contain red algae, foraminifera, echinoids and green algae, with some beds
404 organized into hummocky cross-stratification. Some patch reefs with several coral genera
405 locally occur (Fig. 6D). The breccias consist of angular cm- sized debris of coral reef and
406 bioclastic deposits. Planktonic foraminifera indicate that the lowermost part of this
407 sedimentary unit was deposited during the late Serravallian-Tortonian, between 12.8 Ma and
408 8.2 Ma. Above, foraminiferal assemblages point to Zones N14 to N19 (Tortonian to possibly
409 Zanclean, 11.6-3.8 Ma). The foraminifera in the uppermost part of the section point to Zone
410 N19 and were deposited during the Zanclean, between 5.33 Ma and 3.8 Ma. The perireefal

411 blocks of the breccias originated from two different sources: some developed laterally to
412 patch reefs (Fig. 6D); others were eroded from the underlying late Burdigalian coral complex.
413 Langhian to lower Serravallian deposits were not identified in St Martin, which could then
414 indicate a depositional hiatus.

415 3. **1 to 3 m- thick cross-bedded packstone with red algae and foraminifera**, resting
416 on a subaerial erosive surface (Fig. 6E). The foraminifera found in these deposits point to
417 Zone N19 (Zanclean, 5.33-3.8 Ma).

418 In the southwestern part of St Martin, the Aquitanian-Burdigalian deposits comprise
419 different depositional settings (Fig. 5). To the West (Terres Basses), we found high-angle
420 dipping coral rubble beds overlain by low-angle dipping coral build-ups. This area is
421 interpreted as the outer slope of a coral system, probably set up on the flanks of a late
422 Oligocene subaerial volcano. In the Sabannah area, the occurrence of m- high patch reefs with
423 branching colonies, planktonic and benthic foraminifera, is interpreted as a reef to foreef zone
424 in an open sea (BouDagher-Fadel, 2008; Montaggioni and Braithwaite, 2009). At Mullet Bay,
425 packstones with red algae and benthic foraminifera (amphisteginids and *Asterigerina*) and
426 some coral beds and crossbedding occur, indicating inner-ramp, reefal deposits. In the Juliana
427 Bay and Kool Hill sections, coral banks and benthic foraminiferal assemblages are indicative
428 of a quiet lagoonal depositional environment (Andréieff et al., 1988; Tucker and Wright,
429 1990; BouDagher-Fadel, 2008). To the east of St Martin, the data of Andréieff et al. (1987;
430 1988) indicate the presence of coral reefs at Pinel Islet and on islets east of Phillipsburg. As a
431 result, St Martin was an island during the early Miocene, bordered by coral reef formations
432 with lagoons to the southeast and fringing reefs to the northeast. Langhian deposits were not
433 found, suggesting a possible middle Miocene emersion. Deposition of the upper Serravallian–
434 Tortonian sediments of St Martin (Cupecoy) first occurred in a mid-outer-ramp environment
435 above the Burdigalian reefal deposits indicated by abundant pelagic microfossils. These

436 deposits change upward into mid to inner ramp settings with coral patch-reefs, and associated
437 reefal breccias during the Messinian and the early Zanclean. Zanclean erosional surfaces
438 affect the deposits, indicating a shallowing upward trend ending with an emergence. In this
439 area, the occurrence of reworked breccias from Burdigalian reefal deposits testifies
440 for indicates the permanence of emerged areas.

441

442 5.1.3. Tintamarre

443 At Tintamarre, the deposits are dominated by clayey limestones that yielded abundant
444 macrofauna and larger benthic foraminifera dominated by *Lepidocyclina*, *Miolepidocyclina*,
445 *Miogypsina* and *Amphistegina* associated with planktonic foraminifera. On the basis of six
446 outcrops (Appendix E), the succession comprises, from bottom to top (Fig. 8):

447 1. **13 m- thick packstones** with bivalves (oysters, *Amusium*, *Chlamys*), echinoids
448 (*Clypeaster* and scutellids), larger benthic foraminifera, and some coral debris. The
449 microfossils from the upper part of this unit correlate with the early part of Zone N8 (late
450 Burdigalian);

451 2. **11 m- thick matrix-supported lower megabreccia** with reefal to perireefal clasts
452 (Appendix D; Fig. 9A). Clasts are cm to m- sized with blocks reaching 3 m wide, embedded
453 into a lime wackestone matrix displaying slump structures and forereef-derived bioclasts
454 (*Clypeaster*, larger benthic foraminifera, red algae, and molluscs). Reworked blocks do not
455 display emersion features;

456 4. **0 to 4 m- thick brown clays with gypsum crystals**. This facies, found only in the
457 TINT 10 locality on the northern coast of the island laterally pinches on top of the
458 megabreccia (Appendix D). The three previously described units are yellow to orange in the
459 field, locally brown;

460 5. **33 m- thick wackestone with packstone and breccia interbeddings.** Wackestones
461 mostly yielded bivalves (*Amusium* and other pectinids), echinoids (*Clypeaster*, scutellids), and
462 benthic foraminifera. Packstones are unsorted, mm- to cm- grain-sized, debris-flows with
463 well-preserved pieces of corals, red algae and molluscs. A hummocky cross-stratification is
464 locally found into the packstones. The breccia is composed of cm- grain-sized reworked reefal
465 to perireefal limestones. The succession is tilted to the SE below an erosional surface
466 (Appendix E). The lower 19 m of the lithological succession is green and contains
467 microfossils pointing to Zones N6-N8 (late Burdigalian, 18-15.97 Ma); the upper 14 m is
468 white and microfossils point to Zones N8-N11 (Langhian, 15.9-13.6 Ma).

469 6. **Up to 11 m- thick calcareous upper megabreccia** (Fig. 10). This megabreccia rests
470 unconformably on an erosional surface that transects previously tilted deposits (Appendix E).
471 It is composed of dm- to m- sized transported blocks of coral reef and associated bioclastic
472 deposits and rafted red algae and coral limestone beds reaching several tens of meters long
473 and up to 5 m- thick (Appendix E; Fig. 9A, B). The blocks are embedded into a white to pink
474 wackestone matrix. The megabreccia is crosscut by shear zones and displays numerous soft
475 sediment structures, slump, recumbent folds, isoclinal folds and balls and pillows (Fig. 9C;
476 Appendix E). Shear zones and slumps are indicative of a transport direction to the S-SE. The
477 reefal and red algal-coral rafted beds and clasts yielded benthic foraminiferal assemblages of
478 Zones N5-N8a (latest Aquitanian-Burdigalian; e.g., samples CSM 42, 70 and 71; Appendix
479 E). The matrix yielded planktonic foraminifera further indicating Zone N8b (early Langhian,
480 15.4-15 Ma). Consequently, the upper megabreccia deposited during the early Langhian and
481 comprises reworked Burdigalian limestones.

482 In Tintamarre, Burdigalian to lower Langhian deposits are dominated by clayey
483 limestones that provided shallow-water fauna and debris flow interbeddings with transported
484 corals. Two megabreccias with rafted beds and slumps also occur. The depositional setting is

485 interpreted as an open sea, muddy forereef slope testified by abundant and well-preserved
486 coral fragments (Fig. 8). During the late Burdigalian, however, lagoon conditions temporarily
487 existed with the deposition of gypsum clays above the lower megabreccia. This indicates that
488 the forereef slope depositional setting temporarily turned to shallower conditions then. The
489 upper megabreccia comprises Burdigalian debris and rafts, which were emplaced in a muddy
490 forereef environment during the early Langhian (15.4-15 Ma) (Appendix E; Fig. 9). This
491 megabreccia unconformably lies upon southeastward tilted and eroded early Langhian beds.
492 The blocks of the upper megabreccia do not display any emergence or tectonic features. This
493 indicates that both their destabilization and transportation have occurred under submarine
494 conditions, as classically seen in submarine active tectonic settings where large scale mass
495 wasting is reported (e.g., Hine et al., 1992; Zachariasse et al., 2008; Dailey et al., 2019). The
496 upper megabreccia was transported towards the ESE to SE, indicating that it originated from
497 the WNW to NW in the submerged part of the Burdigalian reefal platform of Anguilla. One
498 way to explain this arrangement is to consider that normal faults trending NE-SW and
499 deeping NW occurred at that time between Anguilla and St Martin, this type of fault having
500 been identified in the southwestern part of St Martin (Legendre, 2018).

501

502 5.1.4. *Barbuda*

503 The Highland Fm. comprises a 30 m- thick carbonate succession. The lower part of
504 the formation does not crop out. From bottom to top we identified (Appendix F):

- 505 1. **4.5 m- thick grainstones with isolated massive, coral colonies.** Corals are dominated
506 by *Montastraea* and *Porites*. The sediments yielded benthic foraminifera (*Miarchaias*, and
507 *Amphistegina*) pointing to the late Miocene;
- 508 2. **9 m- thick red algal and larger benthic foraminifera-rich wackestones to**
509 **packstones;**

510 3. **3.5 m- thick wackestones with some isolated coral colonies** and benthic and
511 planktonic foraminifera (*Neogloboquadrina acostaensis*, *Sphaeroidinellopsis subdehiscens*,
512 and *Globorotalia margaritae*) indicative of a Zanclean age;

513 4. **12.5 m- thick red algal wackestones to packstones with benthic and planktonic**
514 **foraminifera.** The uppermost part of the succession is severely weathered. Planktonic
515 foraminifera indicate that the lower and upper parts of the unit was deposited during the
516 Zanclean and between the Zanclean and Piacenzan, respectively.

517 In Barbuda, benthic foraminifera are dominated by amphisteginids. Mud and planktonic
518 foraminifera occur throughout the section. Corals are documented as isolated, and consist of
519 massive colonies in life position. Consequently, the depositional environment is interpreted as
520 an open-sea, shallow water reefal to foreereef muddy carbonate platform or ramp deposited in
521 low-energy conditions. These results are in agreement with those of Brasier and Donahue
522 (1985), who estimated a palaeobathymetry of *ca* 40-50 m. The middle part of the section is
523 dominated by planktonic foraminifera facies devoid of corals, indicating a deeper
524 environment of deposition than the lower and upper parts of the section. This suggests that the
525 succession has recorded a regressive-transgressive cycle (Appendix F). During the late
526 Miocene-Zanclean interval (samples BAR 1 to 9; Appendix F), the depositional environment
527 changes from reefal inner-ramp (*ca* 10-20 m palaeodepth) to outer-ramp (*ca* 40-50 m
528 paleodepth). The maximum palaeodepth is reached between samples BAR 9 and 13 and
529 occurred during the Zanclean, when wackestones with abundant planktonic foraminifera were
530 deposited. Above, outer-ramp environment changes into mid-ramp during the Zanclean-
531 Piacenzan (?), thereby indicating a moderate regressive trend.

532 5.1.5. Antigua

533 The lowest marine limestone beds of the Antigua Fm. yielded Rupelian foraminifera
534 (*Eulepidina undosa*, *Lepidocyclina* (L.) *urnagunensis*) (Appendix G), while the limestones

535 above them contained Chattian foraminifera (*Lepidocyclina (Lepidocyclina) yurnagunensis*,
536 *L. (Nephrolepidina) braziliana*, *Heterostegina israelskyi*, and *Neorotalia* sp.) (e.g., Pares
537 cross-section; Appendix G.). Consequently, the Antigua Fm. is likely to have been deposited
538 between the Rupelian and the Chattian.

539 In Antigua, the Central Plain Group was deposited into lakes and coastal lagoons, as
540 previously documented (e.g., Martin-Kayes, 1959; Frost and Weiss, 1979; Donovan et al.,
541 2014). Above, the Antigua Fm. was deposited along a low-angle northeastward dipping
542 carbonate ramp, with inner-ramp, reefal environments in the southwest changing
543 northeastwardly into a mid-ramp depositional setting characterized by abundant planktonic
544 foraminifera. These results are in agreement with the regional sedimentary organisation
545 proposed by Martin-Kaye (1969).

546

547 **5.2. Offshore**

548 The profiles GA 11, GA 15, ANT019-24, CPEM 302, CPEM 509 and CPEM 510 are
549 used to compare onshore data with offshore ones because: 1) GA 15 intersects the seismic
550 profile C2 of the Saba Bank petroleum prospect, which was calibrated using wells SBD1 and
551 SBD2 (Matchette-Downes, 2007); 2) GA 11 allows following seismic sequences to the north
552 across the Kalinago Basin; 3) ANT019-24 allows investigating the northwestern margin of the
553 Anguilla Bank; 4) CPEM 302 provides information about the southern part of the Anguilla
554 Bank and allows correlations with the southern part of the Kalinago Basin; and 5) CPEM 509
555 and CPEM 510 illustrate the seismic stratigraphy of the Antigua Bank. In addition, the
556 northern ends of lines GA 08 and GA 09 are only 5 km away from the island of St Martin
557 (Appendix J), 213A was performed on the Anguilla Bank south of St Barthélemy (Appendix
558 J), and 509-510 are located in the vicinity of the island of Antigua, allowing onshore-offshore
559 correlations.

560

561 *5.2.1. Seismic sequences*

562 We identified seven seismic megasequences bounded by regional prominent
563 unconformities and their correlative conformities (Vail et al., 1977; van Wagoner et al., 1988;
564 Cattuneanu, 2006) over the whole investigated area (MS1 to MS7). The most complete
565 succession is best exemplified south of the Saba Bank, along crossing lines GA 15 (ENE-
566 WSW; Fig.10A) and Saba Bank C2 (NW-SE; Fig. 10B). The C2 line was reinterpreted and a
567 seismic pattern partly similar to that of Church and Allison (2004) was found, thereby
568 allowing chronostratigraphic assignments to the megasequences. From bottom to top they are:
569 - **Megasequence 1 (MS1)**: it comprises poorly-defined, chaotic reflectors, locally overlaid by
570 low to very low frequency, discontinuous reflectors. Transparent facies also occur. The top of
571 the sequence is an erosional unconformity termed SB1 usually underlined by a strong
572 amplitude reflection. In wells SBD1 and SBD2, MS1 is overlaid by a subaerial andesitic lava
573 flow that occurred during the late Eocene (38.1-35.9 Ma interval; Church and Allison, 1984).
574 MS1 is found on the GARANTI and ANTITHESIS lines (Figs. 10 to 12; Appendix J) and on
575 the CPEM lines, especially in the southern part of the Kalinago Basin (Fig. 13).

576 No accurate information about MS1 is available yet. Nevertheless, reworked
577 Cretaceous and Paleocene microfossils have been found in the overlying megasequence MS3,
578 suggesting that MS1 is partly made of sedimentary rocks of these ages.

579 - **Megasequence 2 (MS2)**: it comprises seismic units displaying inverted half-graben
580 structures with faint and subparallel to fan-shaped reflectors (Fig. 10A and B). In some cases,
581 it is organized into fan-shaped reflectors draping underlying topographic highs and thickening
582 downward (Fig. 11A; 12). The half-grabens are visible on NE-SW profiles (fig. 10B) and not
583 on NW-SE profiles (Fig.10A), suggesting that their orientation is overall NW-SE. MS2 has
584 not been reached by the drillings. The top of MS2 is the irregular, erosional, newly defined

585 surface SB2 found extended below the late Eocene subaerial andesite drilled in the Saba Bank
586 (Church and Allison, 1984). MS2 has not been recognized in the southern part of the Kalinago
587 Basin (Fig. 13). MS2 probably consists of sedimentary deposits lying unconformably on MS1
588 (Figs. 10A, 11A). It underwent a late mid-Eocene compression leading to inversion of half
589 grabens (Philippon et al., 2020a).

590 - **Megasequence 3 (MS3)**: it comprises up to 2.5 second two-way travel-time (stwt)- thick
591 deposits. MS3 is characterized by discontinuous to continuous reflectors of low amplitude,
592 medium to high frequency, always sub-parallel and well stratified, locally prograding (Fig.
593 10). MS3 onlaps above SB2 and seals the compressive deformations in MS2. It is marked by
594 an abrupt change in seismic facies that evolves from continuous well-bedded reflectors, low-
595 angle truncations in MS2 to onlaps in MS3. The top of the sequence is covered by an
596 unconformity hereafter named SB3. MS3 was not identified in the southern part of the
597 Kalinago Basin (Fig. 13).

598 In the northern part of the Kalinago Basin, MS3 displays regular, mid-amplitude and
599 parallel reflectors (Fig. 10) that progressively pinch against spurs (Fig. 10A, 11A). On lines
600 GA-08 and 09, MS3 displays prograding beds on the southern margin of the Anguilla Bank, a
601 pattern that is also found on lines ANT 19 and 24 (Fig. 11B; Appendix J). These prograding
602 beds are related to downslope detritus originating from the topographic highs. Along the
603 flanks of the spurs, the beds of MS3 are organised into fans mimicking the shape of the relief
604 and down-lapping above unconformity SB2, controlled by NW-SE trending syn-sedimentary
605 faults (Figs. 11A and 13; Appendix J). On the Walichi Flat, south-southwestward prograding
606 beds develop above the basement (Fig. 12B). Offshore in the Antigua Bank and the southern
607 part of the Kalinago Basin, MS3 is missing (Fig. 14). Onshore, continental deposits are
608 recorded (Central Plain Group of Antigua). These observations indicate that the Kalinago
609 Basin was not extending in this area (Fig. 13). Consequently, MS3 has been deposited into

610 sub-basins separated by topographic highs. As no recent fault was evidenced on the margins
611 of the Kalinago Basin, the difference of elevation between the top of the Anguilla Bank and
612 the MS3 deposits of the Kalinago Basin varies between 1,000 to 1,500 m, broadly reflecting
613 the palaeobathymetry of the deep parts of the basin. Such a difference in elevation is also
614 found in the southeastern part of the Saba Bank (Fig. 10).

615 In summary, MS3 unconformably resting upon the erosional surface SB2 is characterised
616 by high relief changes with topographic highs (Walichi Flat, Saba Bank, and spurs) and
617 newly-formed depocentres controlled by synsedimentary normal faults (northern Kalinago
618 Basin).

619 - **Megasequence 4 (MS4)**: it comprises up to 2.5 stwtt- thick gently-dipping reflectors, locally
620 organized into low angle inclined prograding units (Figs. 10 to 12). Onlaps are present against
621 paleoreliefs (Appendix J). The sequence ends with an erosional surface termed SB4 that
622 truncates the underlying reflectors. Locally, low angle reflectors of the overlying
623 megasequence onlap onto SB4. Opposite to MS3, MS4 occurs regionally, from the Kalinago
624 Basin in the NW (Figs. 11, 12) to the Antigua Bank in the SE (Fig. 13).

625 Northeast of Saba Bank, deposition of MS4 is controlled by synsedimentary faults in
626 the NW-SE direction. (Fig. 11A). Southeast of the Saba Bank, MS4 displays parallel bedding
627 (Fig. 10) or fans (Fig. 11A), above the unconformity SB3. In the vicinity of the submarine
628 spurs (Anguillita, Southeastern seamounts) and highs (Saba Bank, Anguilla Bank, and
629 Walichi Flat), SB3 is erosional with toplaps in the underlying MS3 and onlaps in the
630 overlying MS4 (Figs, 10, 11, 13; Appendix J). In the southern part of the Kalinago Basin and
631 Antigua Bank, MS4 directly overlies MS1. Consequently, MS4 is deposited on a topographic
632 surface SB3 which is erosional, except in the deepest parts of the depressions. SB3 exhibits an
633 erosive character over *ca* 500 m vertical drop at maximum, and consequently sedimentation in
634 troughs occurred at several hundred meters depth.

635 - **Megasequence 5 (MS5)**: it reaches 1 stwtt- thick and comprises medium to strong
636 amplitude, medium frequency, parallel continuous reflectors. The sequence shows an
637 aggrading pattern and retrogrades on older reliefs. The top of MS5 is characterised by an
638 unconformity termed SB5. SB5 is either erosional (Fig. 10A, northern part) or bedding is sub-
639 parallel with low-angle onlaps above (Fig. 10B, Saba Bank). MS5 is found from the Kalinago
640 Basin in the NW (Fig. 11, 12) to the Antigua Bank in the SE (Fig. 13).

641 In the Kalinago Basin, South of the Saba Bank, Walichi Flat and Antigua Bank, MS5
642 is organised into parallel reflectors mostly parallel to MS4 reflectors. Onlaps are found in the
643 vicinity of submarine highs, above SB4. The latter displays clear erosional features on the
644 spurs, on the margin of the Anguilla Bank, on the Walichi Flat and on the uppermost part of
645 the Saba Bank (Figs. 10, 11, 12). Consequently, SB4 is interpreted as a subaerial structure
646 developed on submarine highs, that is confirmed by the analysis of the dredged GA 03 rock-
647 samples collected on the southeastern spur (Fig. 2; Appendix I; see below). Erosion is found
648 over a few hundred meters depths at maximum, suggesting that deposition of MS5 occurred at
649 several hundred-metres depth in basin areas.

650 - **Megasequence 6 (MS6)**: it reaches 0.5 stwtt- thick and comprises medium- to strong-
651 amplitude, medium-frequency, continuous and parallel reflectors and prograding reflectors.
652 On the Saba Bank, reflectors are parallel and strongly reflective (Figs. 10, 11), like on the
653 Anguilla Bank and the Antigua Bank (Fig. 13). In the southern part of the Kalinago Basin,
654 MS5 is locally overlain by an erosional surface termed SB6.

655 - **Megasequence 7 (MS7)**: it is distinguishable in the southern part of the Kalinago Basin and
656 Antigua Bank on CPEM seismic lines (Figs. 2, 13). It comprises medium- to strong-
657 amplitude, medium-frequency, continuous and parallel reflectors which locally display fan
658 shaped structures. In the northern part of the investigated area, SB6 is parallel to reflectors

659 and both MS6 and MS7 are often indistinguishable. Consequently, they are grouped into a
660 MS6+MS7 megasequence (Fig. 10).

661 In most of the investigated area, deposits of MS6 and MS7 conformably cap those of
662 MS5. Erosional features are found in the vicinity of spurs (Anguillita and Martinita
663 seamounts) and on Walichi Flat where SB5 displays truncations of the underlying MS5 (Fig.
664 11). Discrete onlaps of fan-shaped reflectors of MS7 above SB6 are found in the southern part
665 of the Kalinago Basin, partly related to the synsedimentary activity of recent normal faults
666 (Fig. 13).

667

668 5.2.2. *GARANTI dredged samples*

669 Dredged samples have been collected on the flanks of seamounts in the northwestern part
670 of the Kalinago Basin and are localized on seismic profiles to allow calibrating the seismic
671 stratigraphy (Fig. 2): DR GA-04-01 and DR GA-04-02 are located on the seismic profile
672 GA11 and DR GA-03-01 on GA13.

673 Dredge DR GA-04-01 (Fig. 11), in MS6, yielded bioclastic wackestones to packstones
674 with red algae and benthic foraminifera. Larger benthic foraminiferal assemblages in these
675 samples correlate with the planktonic foraminiferal zones N14-N18, thus indicating a late
676 Miocene age of deposition (Appendix I).

677 Dredge DR GA-04-02 (Fig. 11), in MS6, yielded wackestones and packstones with
678 planktonic foraminifera. One sample point to Zones N18-N19 (latest Messinian-Zanclean,
679 5.8-3.8 Ma), when another points to Zone N19 (Zanclean, 5.33-3.6 Ma). The wackestones
680 with planktonic foraminifera are bored and borings are infilled with likely modern muds
681 containing planktonic foraminifera of Zones N22-N23 (Calabrian-Holocene).

682 Dredge GA-03-01 in MS5 yielded packstones with red algae and foraminifera pointing to
683 Zones N12b-N20a (Serravallian-Zanclean). The packstones have suffered from

684 microsparitization and are crosscut by opened fractures infilled with wackestones enriched in
685 planktonic foraminifera and reworked microsparitized red algal packstones (Appendix I). The
686 foraminifera found within the wackestones infillings point to Zone N19 (Zanclean).

687

688 **6. DISCUSSION**

689

690 **6.1. Age model**

691 *6.1.1. Onshore*

692 In the Anguilla Bank, the synthetic lithostratigraphical succession of each island can be
693 reconstructed and correlated based on our new biostratigraphic data and field investigations
694 (Fig. 14). In the three islands of the Anguilla Bank, the age of the lower part of the Neogene
695 reefal deposits ranges between the (late?) Aquitanian and the Burdigalian. This age is
696 consistent with i) our new radiometric data at *ca* 25-24 Ma (latest Oligocene) of the andesitic
697 boulder from submarine lahar deposits found below the carbonate platform in St Martin
698 (Appendix K) and ii) that of a subaerial lava flow found in St Barthélemy in a similar setting
699 (Legendre et al., 2018; Cornée et al., 2020) (Appendices G and H). Middle Miocene
700 (Langhian-Serravallian) deposits occur in Anguilla and Tintamarre, but they are missing in St
701 Martin where an erosional unconformity is strongly suspected to have occurred between the
702 Burdigalian and the uppermost Serravallian-Tortonian deposits. However, outcrop conditions
703 did not allow direct observation of this surface. Late Miocene (Tortonian-Messinian)
704 sediments were found in St Martin and Anguilla. In Tintamarre, they may have deposited, but
705 were probably removed by erosion. Zanclean deposits have been identified in St Martin where
706 they are transected by erosional surfaces.

707 In the Antigua Bank and Barbuda, the Highland Fm. encompasses the late Miocene-
708 Piacenzan interval at youngest (Appendix F). Neither unconformity nor major facies change

709 were found between the upper Miocene deposits (samples BAR 1 to BAR 7) and the
710 overlying Zanclean ones. Consequently, a latest Miocene age is considered here (Messinian)
711 for the lower part of the Highland Fm. In Antigua, sediments of the Central Plain Group
712 deposited during the Rupelian (because they are located below the Antigua Fm.), and those of
713 the Antigua Fm. deposited between the Rupelian and the Chattian (Appendix G).

714

715 *6.1.2. Offshore-onshore correlations*

716 Age calibration of offshore sequences and unconformities takes into account the
717 calibration of line C2 with Saba Bank wells, correlations through seismic sequences and
718 unconformities, and dredges data from the GARANTI and other cruises (Fig. 2). These
719 combined data allow calibrating the seismic stratigraphy, correlating onshore and offshore
720 sequences and concur to constrain a late Eocene-Pleistocene age range for the deposits of the
721 Anguilla Bank, Antigua Bank, and Kalinago Basin (Fig. 15).

722 • **MS1:** it correlates with the acoustic basement overlain by a subaerial andesitic
723 complex or MS2. The only chronostratigraphic data available indicate ages ranging between
724 38.7 Ma and 30.8 Ma (Priabonian–Rupelian) in the Saba Bank wells (Church and Allison,
725 2004; Matchette-Downs, 2007). The wells did not reach nor MS1 neither MS2 but yielded
726 reworked Cretaceous and Paleocene microfossils in the sequences overlying the subaerial
727 andesitic complex. Following Jany et al. (1990) and Church and Allison (2004), MS1 is
728 considered to have been deposited between the Late Cretaceous and the middle Eocene.

729 • **MS2:** this locally folded unit (Philippon et al., 2020a) (Fig. 10A) was previously
730 included into the acoustic basement of Church and Allison (2004). It is located between the
731 basement and the Priabonian-Rupelian andesites of wells SBD1 and SBD2, and the overlying
732 megasequence MS3 dating from the late Eocene-early Oligocene. On land at St Barthélemy,
733 compressive structures affecting middle Eocene carbonate deposits (Cornée et al., 2020) have

734 been estimated to have occurred during the late middle-Eocene (Philippon et al., 2020a).
735 Consequently, MS2 and SB2 are assigned to the early middle-Eocene.

736 • **MS3:** it corresponds to the “Lower Carbonate Unit” and the “Channel Turbidite Unit”
737 of Church and Allison (2004) identified on the re-interpreted profile C2 (Fig. 10B). Based on
738 foraminiferal data, the “Lower Carbonate Unit” points to the late Eocene in well SBD1. Based
739 on calcareous nannofossils, the “Channel Turbidite Unit” has been dated to the late Eocene-
740 early Oligocene interval in well SBD2 (Church and Allison, 2004). Consequently, MS3 has
741 an age ranging from the late Eocene to the early Oligocene.

742 • **MS4:** it corresponds to the “Fluvial Deltaic Unit” of Church and Allison (2004) on
743 profile C2 (Fig. 11). This unit yielded microfossils ranging in age from the late Oligocene to
744 the early Miocene (Church and Allison, 2004). On profile GA 08, MS4 can be traced to 5 km
745 off St Martin (Fig. 2; Appendix J). There, MS4 displays progradations and chaotic reflectors.
746 Onshore in St Martin, the margin of the early Miocene carbonate platform is marked by
747 forereef slope deposits which exhibit high dip. (Fig. 6A-B). Moreover, an Oligocene subaerial
748 unconformity was also found in St Martin (Andréïeff et al., 1988; this work) and St
749 Barthélemy (Cornée et al., 2020), between late Eocene and early Miocene deposits. In the
750 Antigua Bank, MS4 partly correlates with the Rupelian-Chattian Oligocene Antigua Fm.
751 Consequently, MS4 deposited during the late Oligocene-early Miocene interval, and the
752 underlying unconformity SB3 is Oligocene.

753 • **MS5:** it corresponds to the lower part of the Upper Carbonate Unit. Foraminifera and
754 calcareous nannofossils indicate that its lower part is not younger than the early Serravallian
755 and its upper part Zanclean at youngest (Church and Allison, 2004). The basal unconformity
756 SB4 is assigned to the middle Miocene and can be traced up to the margin of the Anguilla
757 Bank (lines CPEM 302, GA 08, GA 09; Appendix J). Onshore in St Martin and Tintamarre,
758 this middle Miocene (Langhian) unconformity also occurs, and is overlaid by late Serravallian

759 to Zanclean deposits (Fig. 14). In V-shaped basins eastward in the forearc, Boucard et al.
760 (2021) also described a regional erosional unconformity UB2 between early and middle
761 Miocene sedimentary units. Consequently, MS5 is assigned to the middle-late Miocene and
762 the underlying SB4 unconformity was possibly emplaced during the Langhian.

763 • **MS6:** it corresponds to the upper part of the “Upper Carbonate Unit” of Church and
764 Allison (2004). In the Saba Bank wells, this sequence provided bioclastic coral-dominated
765 deposits covering a red-algal dominated platform. MS6 rests on the erosional unconformity
766 SB5, which corresponds to the base of the reefal deposits still remaining undated. The haul-
767 dredges carried out during the cruise GARANTI on the Martinita and Southeastern seamounts
768 within MS5 and MS6 (Figs. 2 and 11), yielded upper Miocene and lower Pliocene limestones
769 (DR GA 03-01, 04-01, and 04-02; Appendix I). Because microsparitization is found in the
770 upper Miocene limestones, which are also affected by open fractures infilled with Zanclean
771 deposits, we conclude that the Martinita and Southeastern seamounts emerged during the
772 latest Miocene at oldest, and that they subsequently started drowning during the Zanclean.
773 This emersion could relate to SB5. Moreover, the lower Pliocene limestones at site DR-04-02
774 exhibit borings that may indicate that the seamounts were very near sea level or emergent
775 during the Piacenzan-Gelasian interval and were drowned by the Calabrian. These borings
776 could relate to SB6 unconformity. In St Martin, erosional unconformities are found in lower
777 Zanclean deposits (Fig. 6E). In the Guadeloupe Archipelago (*ca* 250 km further south), there
778 is a shallow water carbonate platform that was deposited above a major, latest Miocene to
779 early Pliocene, erosional unconformity (Cornée et al., 2012; Münch et al., 2014; De Min et
780 al., 2015). Red algae-rich deposits dominate in its lower part (Zanclean-Gelasian), and
781 gradually change upwards to coral-dominated deposits (Gelasian-Calabrian). This succession
782 is similar to MS6 in Saba Bank wells. In the Antigua Bank, MS6 was also partly correlated
783 with the Zanclean-Calabrian deposits recovered from the IODP leg 340 (Legendre, 2018).

784 Consequently, the underlying SB5 unconformity is confidently assigned to the latest
785 Miocene-early Pliocene, and MS6 to the early Pleistocene.

786 • **MS7:** it mainly occurs in the southern part of the Kalinago Basin where it is thick
787 enough to be identified on seismic profiles. The wells recovered from IODP 340 indicate a
788 Calabrian (1 Ma) to Holocene age (Coussens et al., 2012). In the northern part of the Kalinago
789 area, MS7 remains thin and was grouped with MS6.

790 In summary, offshore and onshore data allow us to date the Cenozoic deposits in the
791 northern Lesser Antilles, assigning ages to the regional unconformities and estimating the
792 duration of their corresponding hiatuses (Fig. 15): SB1 was emplaced during the Paleocene to
793 middle Eocene ; SB2 during the late Eocene; SB3 during the Oligocene; SB4 during the
794 middle Miocene (Langhian); SB5 during the latest Miocene-early Pliocene; and SB6 during
795 the early Pleistocene.

796

797 ***6.2. Palaeogeographical evolution***

798 Using our dataset that combines onshore and offshore investigations and correlations,
799 we are able to propose novel palaeogeographical maps of the Northern Lesser Antilles (Fig.
800 16). Sequence boundaries on seismic lines were considered subaerial when regional erosional
801 features were observed, with the following criteria: clearly-identified toplaps and onlaps
802 below and above the unconformities, respectively.

803 During the Eocene, the Anegada Passage did not exist (Jany et al., 1990; Mauffret and
804 Jany, 1990). The upper Eocene SB2 unconformity, following an upper Eocene compression
805 (Philippon et al., 2020a), is regionally erosive. MS2 is only preserved as relict patches in the
806 northern part of the Kalinago Basin, Saba Bank and Anguilla Bank, suggesting that SB2 is the
807 expression of a general emersion. The emerged area was extended from the Saba Bank to the
808 Antigua Bank, for at least 300 km, and was connected to Puerto Rico (GraNoLa landmass of

809 Philippon et al., 2020a). In the Anguilla Bank, late Eocene sedimentation resumed after SB2,
810 linked to volcanic activity in St Barthélemy.

811 During the latest Eocene-early Oligocene (MS3) (*ca* 38-28 Ma), to the north of the
812 studied area, a major extensional episode occurred along NW-SE trending faults. The
813 Kalinago Basin opened and the sea invaded the depressions despite the sea level drop of about
814 a hundred meters that occurred at the Eocene-Oligocene transition (Miller et al., 2020). The
815 Saba, Anguilla and Antigua banks and the Walichi Flat remained all above sea level in the
816 footwall of normal faults. At that time, volcanism was active in Antigua, St Martin and St
817 Barthélemy islands, and in Saba Bank (Fig. 16B).

818 During the late Oligocene (SB3) (28-23 Ma), the rifting propagated southward and the
819 Kalinago Basin deepened. Its eastern and western shoulders were uplifted and became
820 emergent in the Saba Bank and from Antigua to the Walichi Flat (Fig. 16C). Onshore, this
821 emergence is clearly recorded: in St Martin, subaerial upper Oligocene volcanism is now
822 proven and Aquitanian reefs developed onto tilted and eroded Eocene sediments (Andréieff et
823 al., 1988; this study); in St Barthélemy, an erosional surface crosscutting the upper Eocene
824 deposits is capped by upper Oligocene subaerial lavas (Cornée et al., 2020); in Antigua, the
825 Rupelian Central Plain Fm. was deposited in an inland paleoenvironmental setting, then the
826 sea invaded the island during the Rupelian and the Chattian.

827 During the latest Oligocene-early Miocene (MS4) (24-16 Ma), only small islands
828 remained above sea-level, despite hundred meters sea level drops, indicating a significant and
829 general subsidence (Fig. 16D). The now drowned but previously emerged area extending
830 from Antigua to Anguilla was then capped by reefal carbonate deposits delineated by steep
831 slopes and their associated deposits. Elsewhere, basin sediments were deposited. Some
832 tectonic activity is recorded in the Anguilla Bank with mass wasting and synsedimentary
833 normal faults in St Martin (Legendre, 2018; this study). A subaerial volcanic activity is

834 evidenced in St Barthélemy and Antigua. Offshore, MS4 infilled depressions or fringes spurs,
835 indicating regional subsidence. Fault activity is recorded only to the north of the study area,
836 on the southern margin of the Walichi flat, in the Kalinago Basin. In the forearc to the east of
837 the Anguilla Bank, steep NE-SW trending fault controlled basins opening (V- shaped basins,
838 Boucart et al. (2021)) (Fig. 1B) (St Barthélemy and Antigua valleys). NW-SE and their
839 conjugated NE-SW trending normal faults were sealed by MS5 (Fig. 10A). In St Martin, the
840 upper Oligocene pluton and its country rock are tilted along NE-SW trending faults
841 (Legendre, 2018). In Anguilla, the Eocene beds were tilted to the SE and capped by a sub-
842 horizontal Miocene carbonate platform, suggesting that the tilt was also controlled by this set
843 of NE-SW trending faults. Consequently, moderate fault activity is found only in the northern
844 part of the investigated area, at the vicinity of the Anegada Trough, which probably started to
845 open.

846 At St Martin in the Juliana airport section (Appendix D), E-W trending synsedimentary
847 normal faults affected the upper Burdigalian lagoonal deposits. These faults display dip-slip
848 kinematics indicating a NNE-SSW extension (Fig. 7) (Legendre, 2018; Noury et al., 2018).
849 Such an orientation is consistent with the Kalinago rift trend. Local uplifts have been recorded
850 during this tectonic episode, at Juliana and Kool Hill, with the occurrence of karstic features
851 (Appendix D). In Tintamarre, the lower megabreccia also was deposited during the late
852 Burdigalian (Fig. 9; Appendix E), and it was likely coeval with the deposition of lagoonal
853 sediments indicative of a temporary uplift (Fig. 14). Consequently, the emplacement of the
854 lower megabreccia is most related to observed strain affecting the Juliana section, both
855 indicating moderate N-S to NNE-SSW extension (*i.e.* parallel to the trench extension) in this
856 area between 18 Ma and 16 Ma.

857 During the early Langhian (SB4) (15.4-15 Ma), the sea level rose by 80 m (Miocene
858 climatic optimum; Miller et al., 2020; Westerhold et al., 2020). Large islands, however,

859 emerged and shallow banks were deposited. This indicates that another significant uplift event
860 occurred, which was most probably controlled by NE-SW faults that tend to be parallel to the
861 Anegada Trough (Fig. 16E). Antigua, southern Anguilla and Saba Banks became emergent
862 whilst the northern Anguilla Bank remained under shallow waters. Elsewhere, basin
863 sediments have been deposited. East of Anguilla Bank, the spurs separating the V- shaped
864 paleovalleys emerged during the early-middle Miocene and underwent erosion (Boucard et
865 al., 2021). Volcanic activity is not recorded onshore neither offshore.

866 Between the middle Miocene and the early Pliocene (MS5) (*ca* 15-4 Ma), a new
867 regional drowning occurred and only small islands were emergent (St Barthélemy and St
868 Martin) (Fig. 16F). From Anguilla to Antigua, shallow water reefal platforms have formed
869 whilst basin deposits occurred elsewhere and the V- shaped basin did not operate anymore
870 (Boucard et al., 2021). On the southern margin of the Anguilla Bank, MS5 locally display
871 chaotic reflectors that could indicate slope deposits (Fig. 13B).

872 During the latest Messinian-early Zanclean (SB5) (*ca* 6-4 Ma), the sea level rose by 20
873 m (Miller et al., 2020) but new islands appeared, indicating a regional uplift (Fig. 16G). These
874 new islands, fringed by shallow-water carbonate deposits, emerged from Anguilla to Antigua
875 and shallow-water reefal deposits were emplaced on the Saba Bank. The volcanic islands of
876 the present-day volcanic arc began to emerge by the Pliocene in northwest St Eustatius and
877 southeast St Kitts (e.g., MacDonald et al., 2000). Elsewhere, basin deposits are observed.

878 During the Zanclean-Calabrian (MS6) (4-1 Ma), glacio-eustatic sea level variations
879 could reach 90 m (Miller et al., 2020). The present-day physiography of the northern Lesser
880 Antilles was mostly acquired (Fig. 16H). A regional drowning has however occurred, of
881 greater amplitude than sea level variations, since only small islands remained emerged (St
882 Martin, St Barthélemy, Anguilla, and Antigua). Eastward in the forearc, a drastic subsidence
883 occurred and is likely to be related to margin basal and frontal subduction erosion, which

884 probably accounts for the retreat of the volcanic arc westward (Boucard et al., 2021).
885 Contemporaneously, the volcanic islands of the recent arc emerged, extending from
886 Montserrat to Saba. Discrete synsedimentary faulting is recorded in the southern part of the
887 Kalinago Basin. On the Antigua, Anguilla and Saba Banks, reefal and red algal platforms
888 were emplaced.

889 During the middle and late Pleistocene, several glaciations occurred, coinciding with
890 recurrent up-to-*ca* 120 m- drops in global sea level (e.g., during Marine Isotopic Stages 16a,
891 12a, 10a, 6a, and 2 [at 0.63, 0.44, 0.34, 0.14, and 0.03 Ma, respectively]; Railsback et al.,
892 2015; Miller et al., 2020; Westerhold et al., 2020) (Fig. 16I). Evidence of emersion has been
893 found in carbonate submarines banks, such as Saba Bank, where giant sinkholes, several
894 hundred meters deep, have been recently revealed (van Duyl and Meesters, 2018). These
895 drops had direct consequences on the emerged areas and relationships between the northern
896 Lesser Antilles islands.

897

898 ***6.3. Geodynamic settings since the late Eocene***

899 The strain pattern observed in this study reflects the accommodation of trench bending
900 that followed a plate boundary rearrangement at the northeastern corner of the Caribbean
901 Plate, which originated both from collision between the Bahamas Bank and Greater Arc of the
902 Caribbean with along its northern boundary and a major change in plate kinematics
903 (Boschman et al., 2014; Legendre et al., 2018; Philippon et al., 2020a, b; Boucard et al.,
904 2021). Our palaeogeographical reconstructions (Fig. 16) allow, for the first time, to evidence
905 regional scale vertical motions affecting the whole northern Lesser Antilles. Indeed, we show
906 the emergence of hundreds km- long landmasses along the trench in the arc area and
907 subsequent regional drownings of these lands at the scale of tens Myrs.

908 Following the E-W compression that occurred during the late-middle Eocene
909 (Philippon et al., 2020a), which led to large emerged areas in the northern Lesser Antilles, the
910 tectonic regime changed drastically. Since then, the palaeogeography has been controlled by
911 regional extensional setting leading to alternating episodes of uplift and subsidence. Vertical
912 motions are controlled by two sets of normal faults trending NE-SW and NW-SE,
913 respectively. The Kalinago Basin opened during the late Eocene-early Oligocene and
914 propagated from north to south, between ~34 and ~28 Ma, in intra-arc rift position (MS3).
915 First, this opening was controlled by NW-SE trending normal faults, *i.e.* parallel-to-the-
916 trench. Later on, NW-SE and NE-SW trending regional normal faults affected the northern
917 Lesser Antilles realm (MS3 and MS4) (Jany et al., 1990; Legendre et al., 2018; Boucard et al.,
918 2021; this work). Consistently, NE-SW-trending faults fractured the inner forearc generating
919 deep V-shapes valleys separated by shallow crustal spurs (Boucard et al., 2021). This regional
920 extension in the upper plate possibly resulted from the Bahamas Bank collision and westward
921 drifting, the consecutive margin convex bending and crustal blocks rotations (Mann et al.,
922 2005; Philippon et al., 2020b). This extension might also be consistent with a transient trench
923 rollback (over a short time lapse) during the early stages of extension. Soon after SB3 (late
924 Oligocene erosional surface), the zone of maximum subsidence switched eastward to the
925 forearc, on the eastern margin of the Kalinago Basin where the V-shaped deep basins and
926 Spurs opened during the late Oligocene-early Miocene (Boucard et al., 2021). Volcanism
927 remained active from Antigua to St Barthélemy, and ceased at *ca* 24 Ma in St Barthélemy and
928 St Martin.

929 Between SB4 and SB5 (middle Miocene-early Pliocene) the deformation regime
930 changed. The tectonic activity along the NE-SW faults, which bound the V-shaped basins, has
931 progressively ceased and deep NW-SE faults resulted from an extensive deformation normal
932 to the margin. A significant subsidence affected the forearc and the Kalinago basin. The

933 volcanic arc migrated westward into the arc interior. The margin has likely undergone a long-
934 term frontal erosion compared to the accretionary Central and Southern Lesser Antilles. This
935 frontal erosion, trench landward migration associated with margin extension, fracturing,
936 drastic subsidence and volcanic arc landward retreat testify for enhanced basal erosion of the
937 upper plate (Boucard et al., 2021).

938

939 ***6.4. Faunal dispersals***

940 Our results indicate that prominent uplift events occurred during the late Bartonian-
941 early Priabonian, the Chattian, the Langhian and the early Zanclean in the northern Lesser
942 Antilles. During these intervals, hundred kilometers- long and wide emerged islands extended
943 from Antigua to the Anguilla and Saba Banks (Fig. 16), thus providing more or less
944 continuous terrestrial connections to the Greater Antilles (Puerto Rico and Virgin Islands).
945 Such a connection has been previously proposed but only for the late Eocene (GrANoLA
946 land, Philippon et al., 2020). Whereas it has been unsuspected until now, with this thorough
947 geological and geophysical study of the Northern Lesser Antilles realm, we evidence that the
948 northern part of the Lesser Antilles has been a favourable area that may have allowed the
949 dispersal of terrestrial species between the Greater Antilles and the northern part of South
950 America, not only during the late Eocene but also from the Oligocene to recent times with the
951 episodic formation of emerged archipelagos. Moreover, this potential transit zone identified
952 here, from the Anguilla Bank to the Antigua Bank, can be extended southwards to the
953 Guadeloupe archipelago where, there too, vast island areas have been identified with a similar
954 schedule: at the early Miocene-middle Miocene transition, at the late Miocene-early Pliocene
955 transition and during the Early Pleistocene (De Min, 2014; De Min et al., 2015), aside from
956 Pleistocene sea-level drops controlled by glaciation (Railsback et al., 2015). Thus, the
957 northern Lesser Antilles might have contributed to faunal dispersals at multiple times since

958 the late Eocene. During the late Eocene, the emerged areas in the northern Lesser Antilles
959 were at their maximum and might have been connected to the supposed GAARlandia land
960 bridge, playing a role in the dispersal of South American terrestrial fauna to the Greater
961 Antilles (Iturralde-Vinent and McPhee, 1999). However, later dispersal events have also been
962 evidenced (Fabre et al., 2014; Brace et al., 2015; Courcelle et al., 2019) and they may be
963 supported by the repeated occurrence of more or less important emerged land masses in the
964 northern Lesser Antilles (this work) and possibly in the southern Lesser Antilles, too. The role
965 of the Lesser Antilles in the dispersal of land fauna during the last 40 Myrs must therefore be
966 reassessed, on one hand by searching for a terrestrial fossil record that is currently lacking,
967 and on the other hand by reconstructing the palaeogeography of its southern part between
968 Guadeloupe and Venezuela.

969

970

971 **7. CONCLUSIONS**

972 Our integrated onshore-offshore study of the Cenozoic deposits of the northern part of the
973 Lesser Antilles shows:

- 974 • An isolated reefal platform in Anguilla lasting the whole Aquitanian to Messinian
975 interval (23-*ca* 5.3 Ma); reefal to peri-reefal deposits fringing an island in St Martin
976 and covering the Aquitanian-Zanclean interval (23-3.8 Ma); peri-reefal to slope
977 deposits at Tintamarre with two episodes of mass wasting, which occurred during the
978 late Burdigalian (18-16 Ma) and the early Langhian (15.4-15 Ma), respectively; reefal
979 deposits at Barbuda from the Messinian-Piacenzan(?) (?11.6-?2.5Ma); reefal then deep
980 sea deposits in Antigua spanning the Rupelian-Chattian interval (?33.9-23 Ma).
- 981 • Offshore, we defined seven seismic megasequences (MS) bounded by regional-scale,
982 erosional unconformities. MS1 corresponds to a partly sedimentary Cretaceous to

983 lower Eocene deformed basement; MS2 is a middle-upper Eocene sequence
984 displaying inverted grabens; MS3 deposited during the late Eocene and the early
985 Oligocene; MS4 deposited between the late Oligocene and the early Miocene; MS5
986 deposited between the middle Miocene and the early Pliocene; MS6 and MS7
987 deposited during the early Pliocene and the Pleistocene.

- 988 • Our palaeogeographical reconstructions highlight uplifts and emergences of hundreds
989 km- long islands during the late Eocene, the late Oligocene, the early Langhian, and
990 the latest Miocene-earliest Pliocene. These uplift events have been interspersed by
991 drowning episodes that occurred during the early Oligocene, the middle Miocene-
992 earliest Pliocene and from the early Pliocene to the present-day. Uplift episodes
993 generated archipelagos with mega-islands and/or neighbouring islands in the Greater
994 Antilles, the Lesser Antilles, and the northern Aves Ridge.
- 995 • A major, first order geodynamical change occurred by the late Eocene (37.8-33.9 Ma):
996 a convergent event occurred during the late middle-early late Eocene (42-37 Ma),
997 related to the collision between the Caribbean Plate and the Bahamas Bank; later, only
998 extension is recorded with alternating uplift and drowning episodes related to an
999 increasing curvature of the trench. The Kalinago Basin opened as an intra-arc basin
1000 during the Priabonian-Rupelian (37-28 Ma). The role of the northern Lesser Antilles
1001 concerning the dispersal of terrestrial organisms, between the Greater Antilles and
1002 northern South America, has to be re-evaluated in the light of our palaeogeographic
1003 reconstructions.

1004

1005 **Acknowledgements**

1006 This work was supported by the INSU TelluS-SYSTER grant call 2017, the
1007 GAARAnti project (ANR-17-CE31-0009), the GARANTI Cruise (2017) and the

1008 ANTITHESIS Cruise (2013). We are indebted to Saba Bank Resources N.V. for the provision
1009 of seismic lines of the Saba Bank area. We gratefully thank the captain and crew of *R/V*
1010 *L'Atalante*, as well as the technical staff of Genavir for having successfully completed the
1011 acquisition of seismic data and dredge samples during the GARANTI and ANTITHESIS
1012 cruises (<https://doi.org/10.17600/17001200>). Multichannel seismic processing was performed
1013 with Geovation software of CGG and Seismic Unix. All geophysical data of the
1014 ANTITHESIS and GARANTI cruise are available on demand at SISMER
1015 (www.ifremer.fr/sismer/). Thin-sections were made by D. Delmas and C. Nevado
1016 (Montpellier) and F. Zami (Pointe à Pitre). Paul Mann, an anonymous reviewer and Editor
1017 Christopher Fieding are thanked for their constructive reviews.

1018

1019

1020

1021

1022

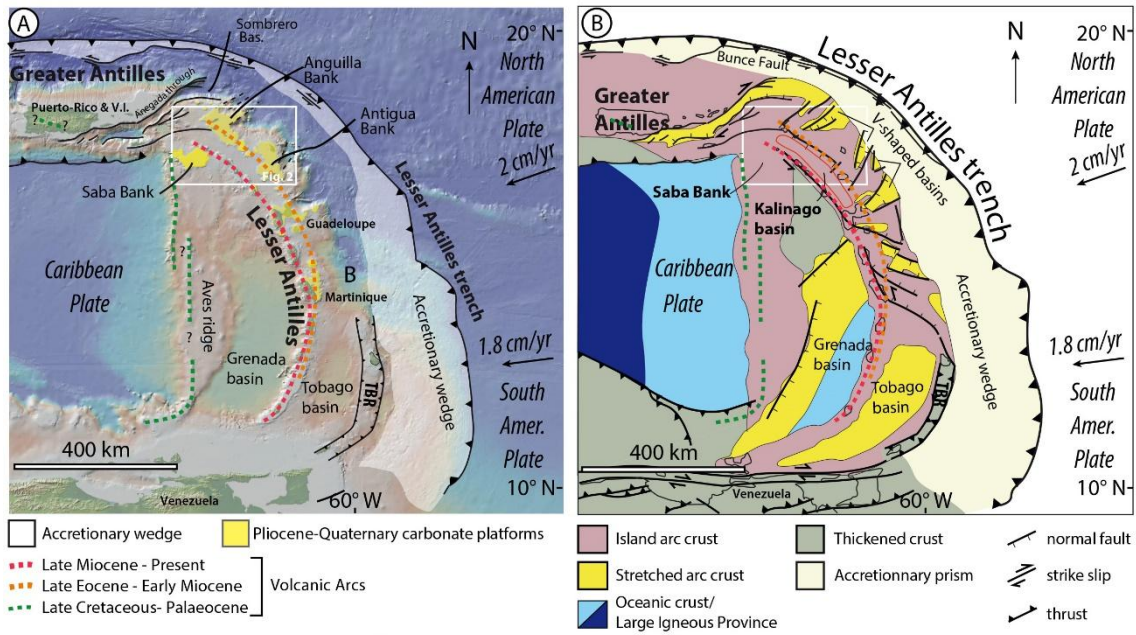
1023

1024

1025

1026

1027 **Figures**

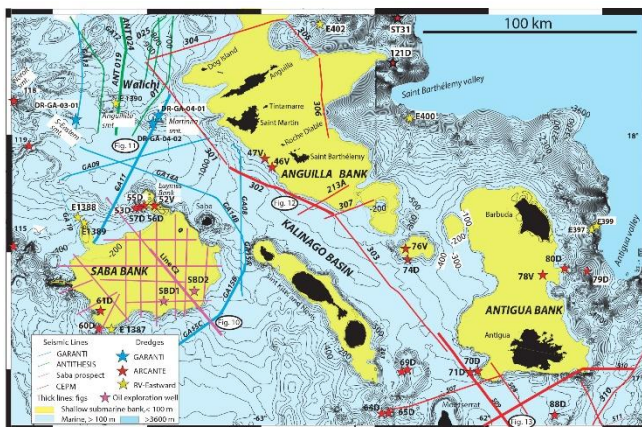


Cornée et al., Fig. 1

1028

1029 Fig. 1: A: tectonic setting of the Lesser Antilles subduction zone; B: schematic map of the
 1030 main crustal blocks; the main faults are drawn from Jany et al. (1990), Feuillet et al. (2002,
 1031 2010), Clark et al. (2008), Gomez et al. (2018), Garroq et al. (2020), Padròn et al. (2020),
 1032 and Boucard et al. (2021). The study area is delineated by the white rectangle. TBR: Tobago
 1033 Barbados Ridge.

1034



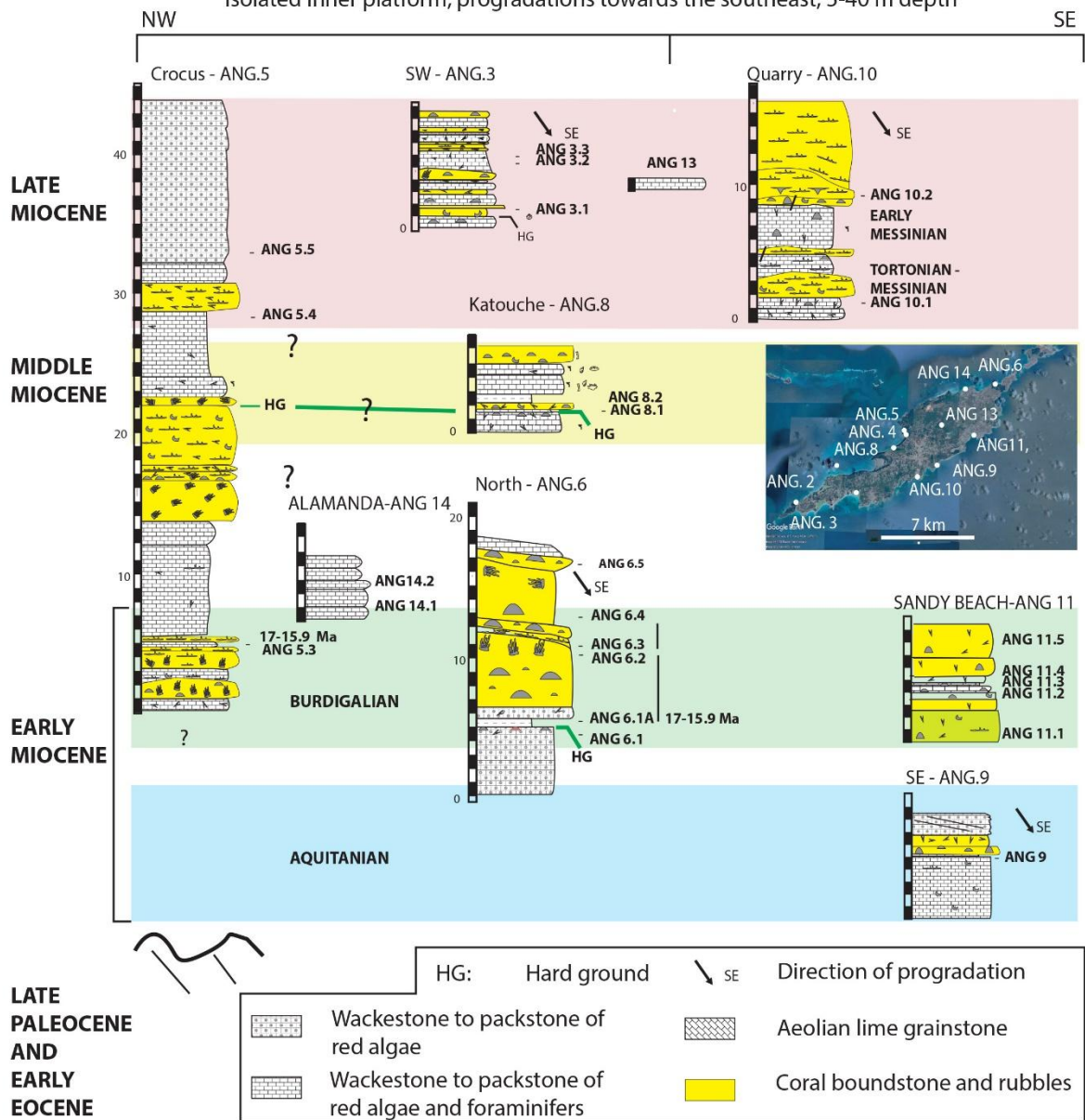
Cornée et al., Fig. 1

1035

1036 Fig. 2: Location of the studied seismic profiles, dredges and investigated islands of Anguilla
 1037 and Antigua banks. Thick lines correspond to seismic lines of figures 10 to 13.

1038

Low energy, shallow reefal, coral banks, flat domes
 Isolated inner platform, progradations towards the southeast, 5-40 m depth

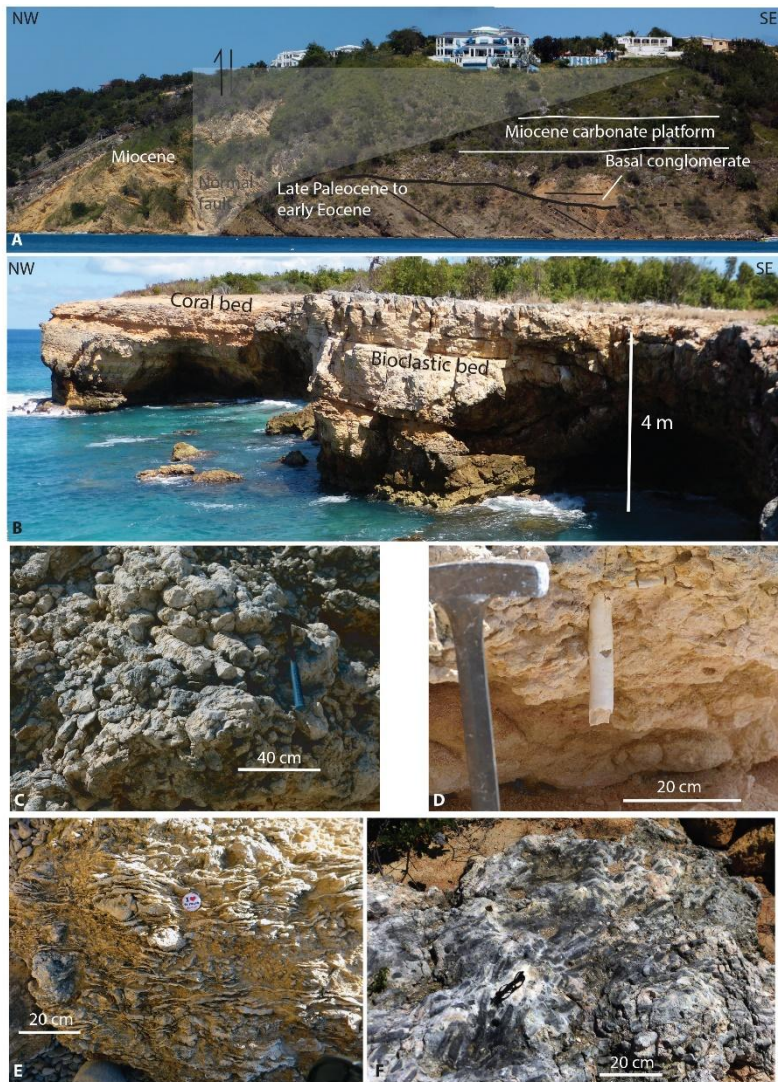


1039 Cornée et al. Fig. 3

1040 Fig. 3: Correlations of the cross-sections in Anguilla. The location, description and
 1041 depositional settings of the sections, as well as the palaeontological content of the collected
 1042 samples are detailed in Appendix C.

1043

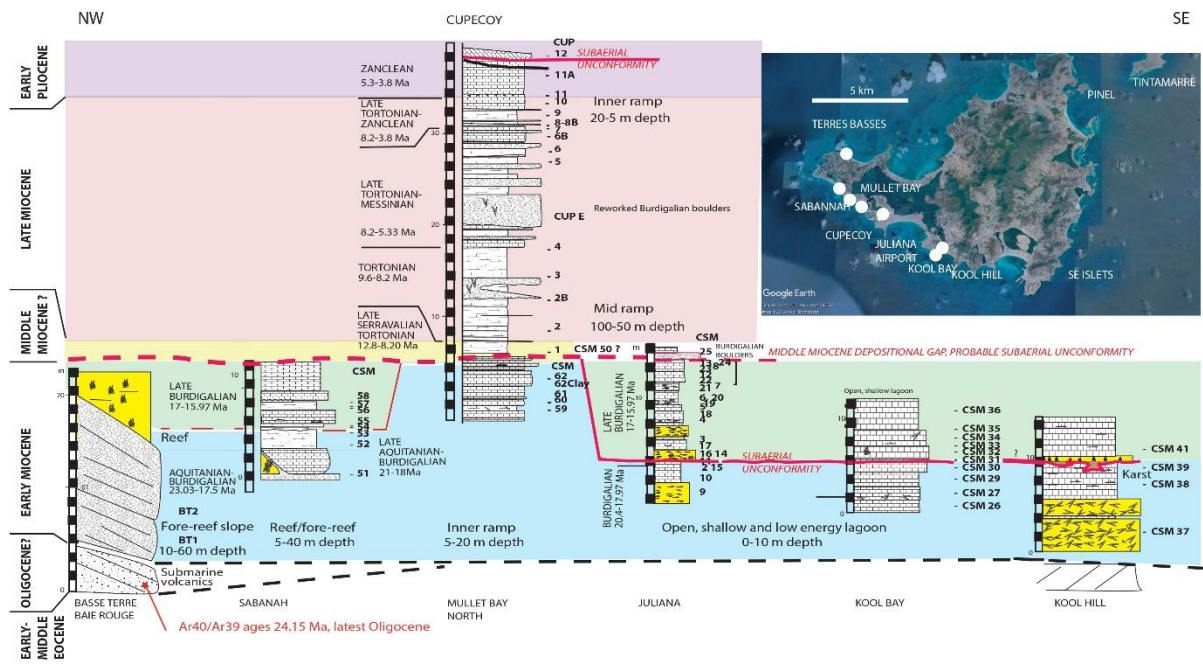
1044



1045 Cornée et al., Fig. 4

1046 Fig. 4: Field view of Anguilla. A: southeastward tilted upper Palaeocene to lower Eocene
 1047 turbidites overlain by sub-horizontal, undated conglomerates then lower Miocene reefal
 1048 carbonates (Crocus Bay); B: typical aspect of the coral and bioclastic banks (locality ANG 3,
 1049 late Miocene; Appendix C); C: detail view of a coral biostromal bed with sub-horizontal thick
 1050 branched *Porites* colonies (locality ANG 6, Burdigalian); D: *Teredo* in life position (locality
 1051 ANG 3, late Miocene); E: sheet-like *Porites* coral colonies with some massive ones (locality
 1052 ANG 10, late Miocene); F: m- high patch reef build-up with branching colonies of
 1053 undertermined genus (locality ANG 3, late Miocene).

1054



1055 Cornée al., Fig. 5

1056 Fig. 5: Correlations in St Martin. The location, description and depositional settings of the
 1057 sections, as well as the palaeontological content of the collected samples, are detailed in
 1058 Appendix D.

1059

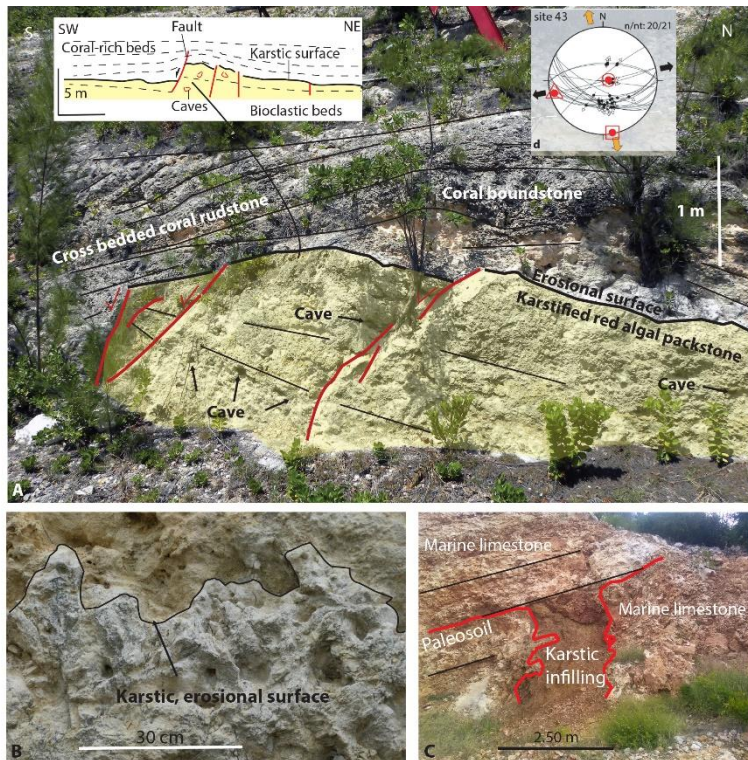
1060



1061 Cornée et al., Fig. 6

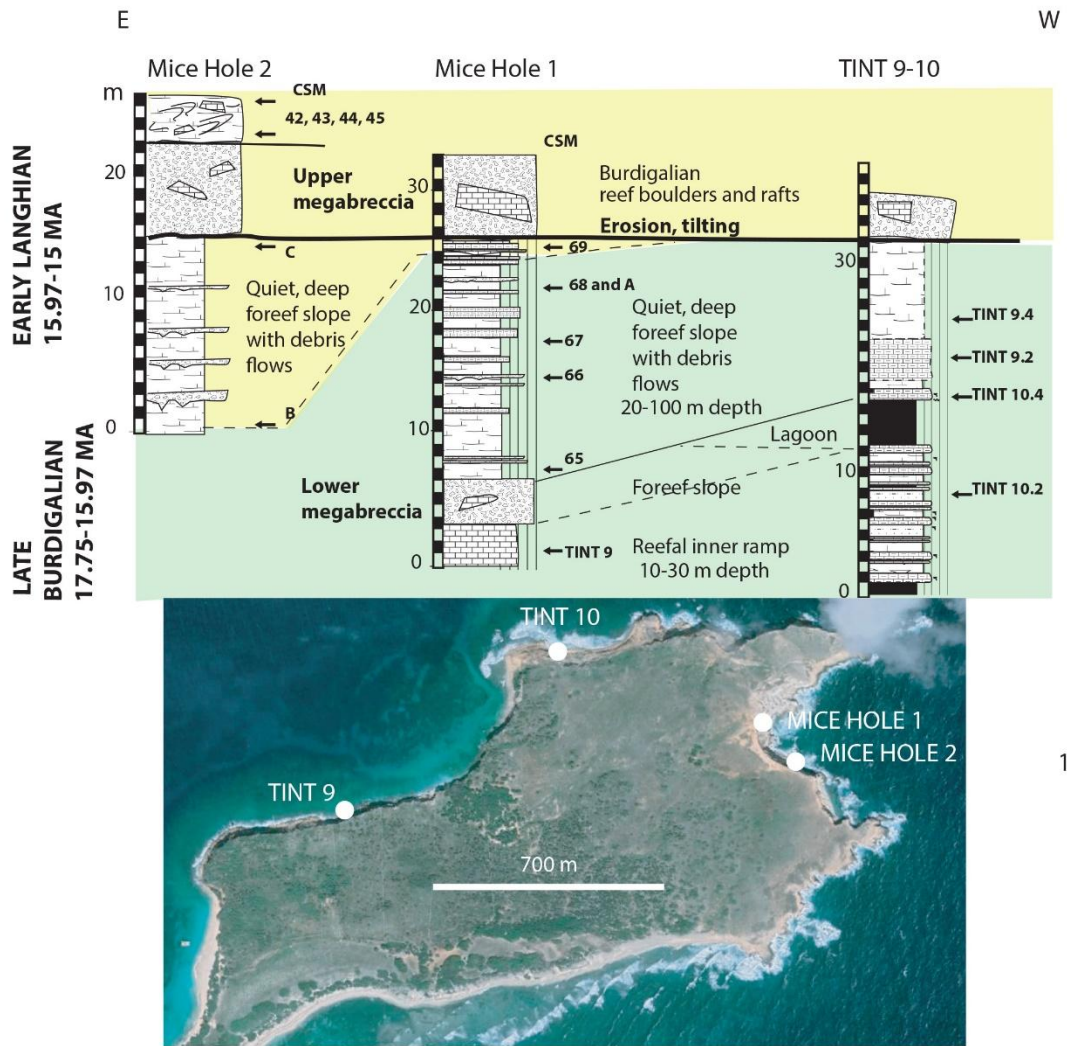
1062 Fig. 6: Field view of St Martin. A and B: lower Miocene reefal/forereef slope deposits
 1063 composed of coral debris above Oligocene lahars (Terres Basses, Baie Rouge; location in
 1064 Appendix D); C: lagoonal, Burdigalian biostromal coral beds (Juliana airport); D: inner ramp
 1065 patch reefs and associated coral breccias, late Miocene (Cupecoy Bay); E: intra-Zanclean
 1066 erosional surfaces (Cupecoy).

1067



1068 Cornée et al., Fig. 7

1069 Fig. 7: Emergence features in the upper Burdigalian deposits. A: synsedimentary normal
 1070 faults in the Burdigalian lagoonal deposits (Juliana airport; stress tensors from Legendre,
 1071 2018). The horst structure is topped by an emersion surface below which microcaves were
 1072 found; B: detailed view of the emersion surface with karstic gullies sealed by the overlying
 1073 deposits; C: palaeosol and karstic cave infilled with red silty clay within Burdigalian reefal
 1074 beds; the cave is sealed by Burdigalian marine bioclastic limestones (southern side of Kool
 1075 Hill).
 1076



10

1077 Cornée et al. Fig. 8

1078 Fig. 8: Correlations in Tintamarre. The location, description and depositional settings of the
 1079 sections, as well as the palaeontological content of the collected samples are detailed in
 1080 Appendix E.

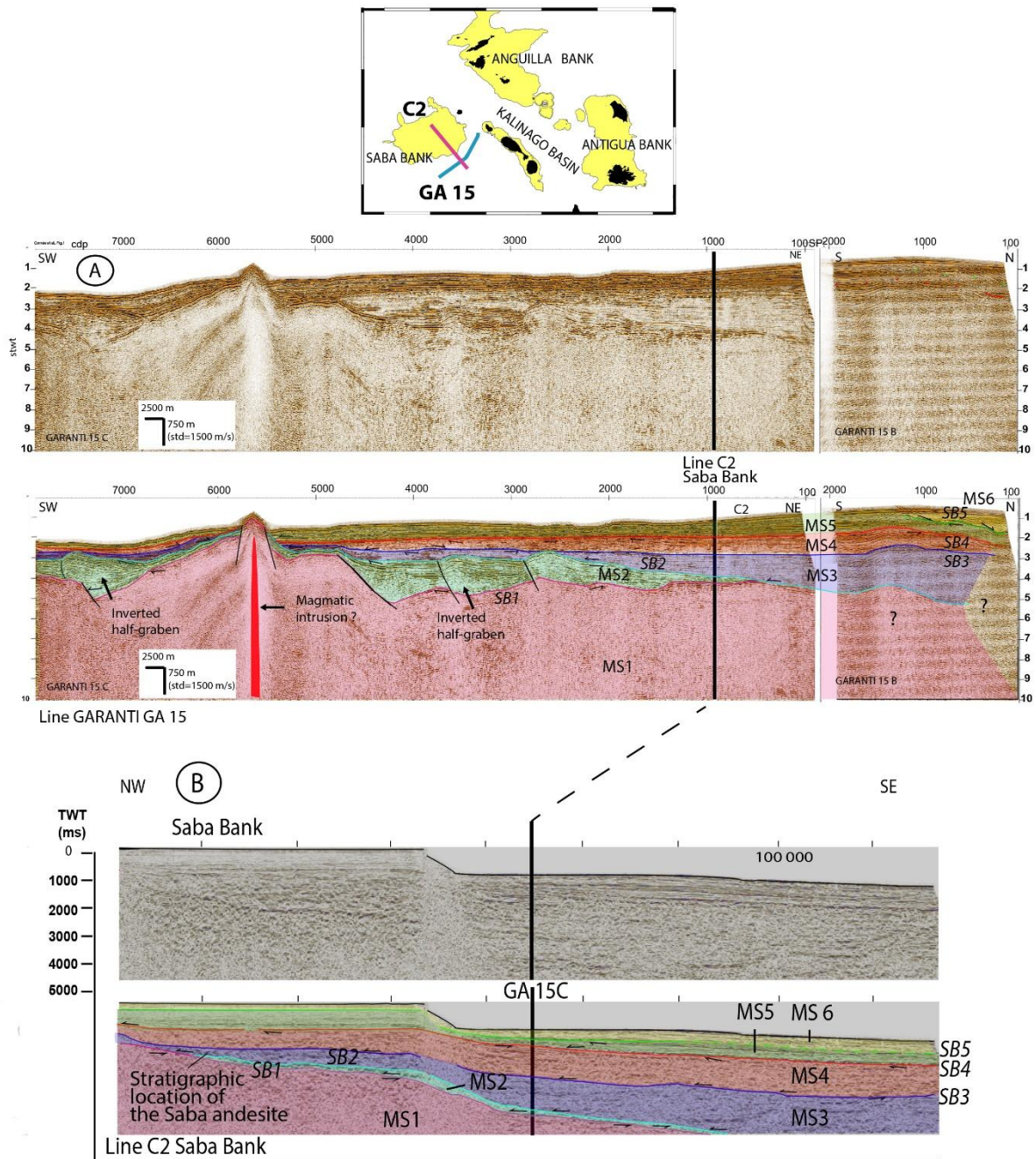
1081

1082



1083 Cornée et al., Fig. 9

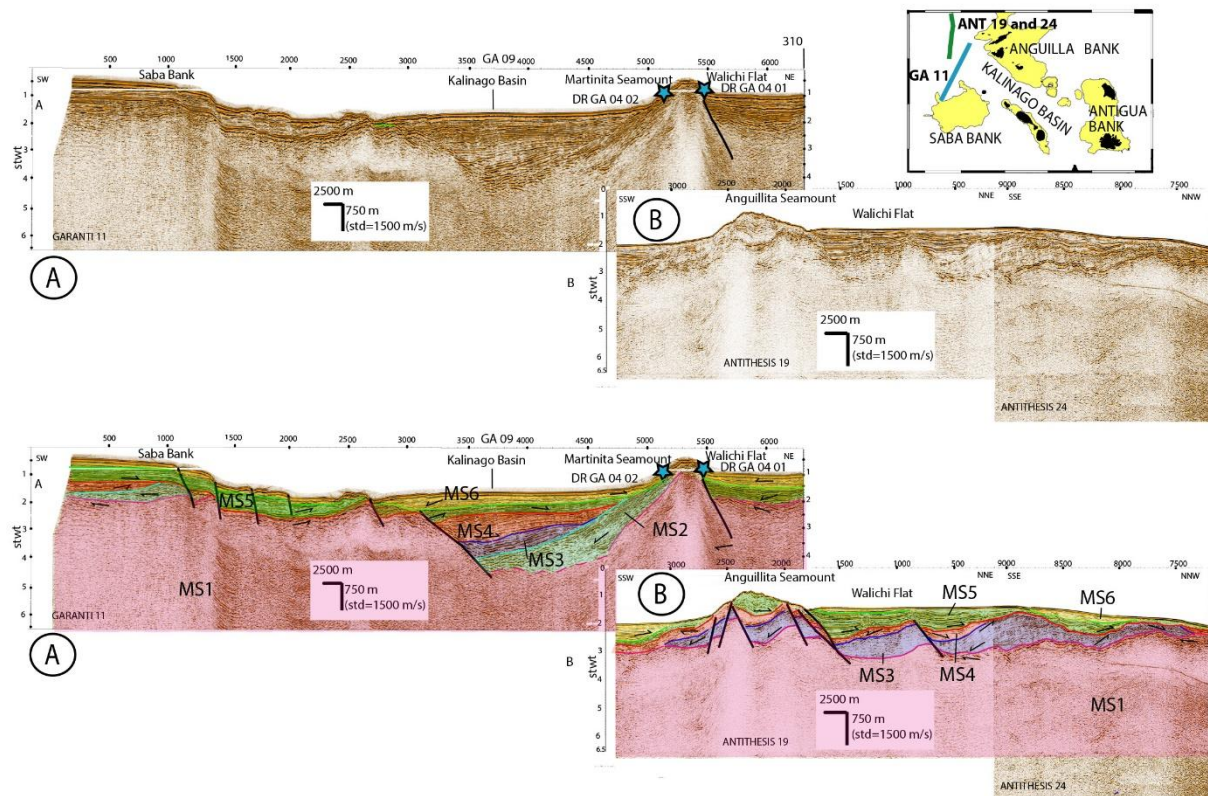
1084 Fig. 9: Megabreccias at Tintamarre, locations in Appendix E. A: lower and upper
 1085 megabreccias with early Miocene (20-16 Ma) rafted blocks into bioclastic forereef slope
 1086 (northern cliff of Tintamarre, 200m west from locality TINT 10). In this area, most of the
 1087 upper Burdigalian and lower Langhian deposits have been removed below the upper
 1088 megabreccia; B: detailed view of the middle Miocene (15.4-15 Ma) upper megabreccia
 1089 consisting of Burdigalian rafted limestone beds and dm- to m- wide blocks (Mice Hole 2
 1090 locality); C: pink, uppermost part of the middle Miocene (15.4-15 Ma) upper megabreccia
 1091 with m-sized block and large isoclinal fold slumps (locality CSM 43).



Units of Church and Allison (2004)	This study North Kalinago	Age of MS	Age of SB
Upper Carbonate Unit	MS6	Early Pliocene-Pleistocene	SB6 E. Pleistocene
	MS5	Middle Miocene-early Pliocene	SB5 Latest Miocene Early Pliocene
Fluvial Deltaic Unit	MS4	Late Oligocene-early Miocene	SB4 Mid Miocene
Andesite then Lower Carbonate and Turbidites Unit	MS3	Late Eocene-early Oligocene	SB3 Oligocene
	MS2	Eocene	SB2 Late Eocene
Cretaceous to Paleocene basement,	MS1	Cretaceous/Paleocene basement	SB1 Early to middle Eocene?

1092 Cornée et al. Fig.10
 1093 Fig. 10: Reference seismic lines. A: GARANTI GA15 line; B: C2 line (Matchette-Downes,
 1094 2007, re-interpreted). MS: megasequence; SB: sequence boundary.

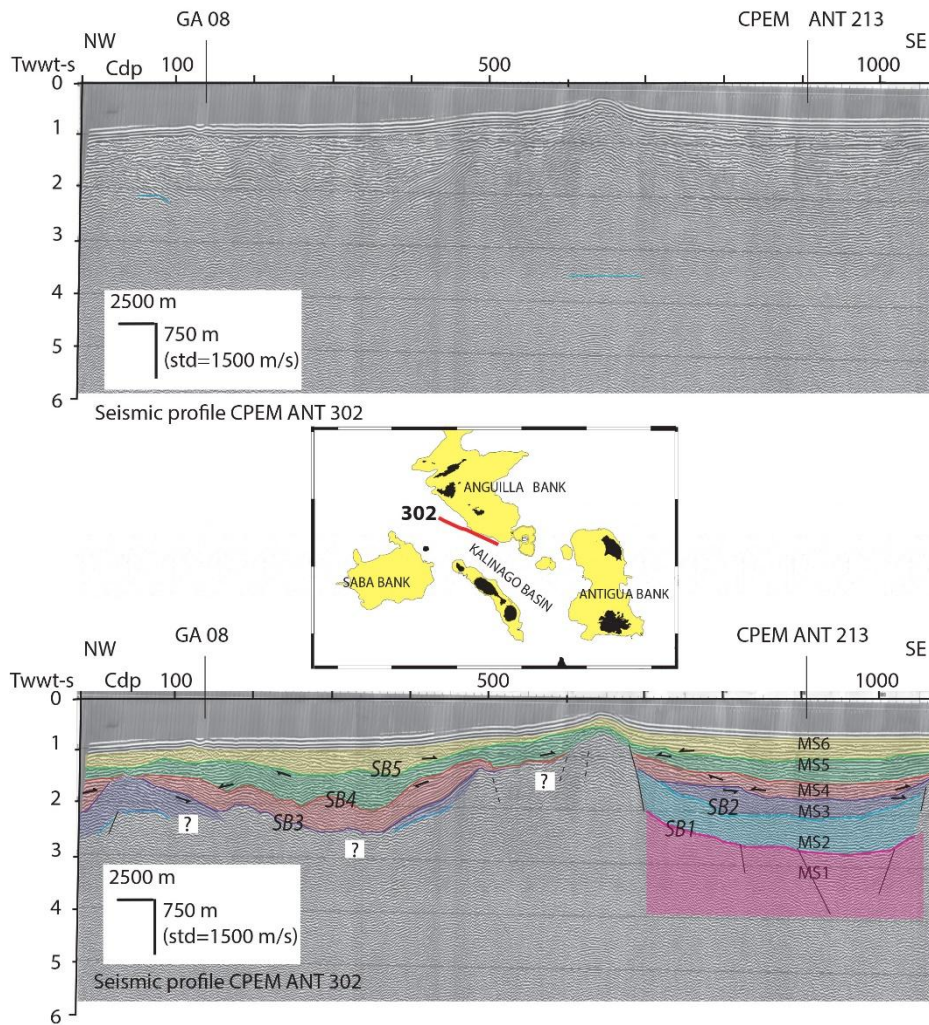
1095



1096 Cornée et al., Fig. 11

1097 Fig.11: A: GARANTI seismic line GA11; B: ANTITHESIS seismic lines 19 and 24. The
 1098 Kalinago Rift opened during deposition of MS3 and MS4, which were deposited into syn-
 1099 sedimentary half-grabens. MS2 is only preserved in the vicinity of the Martinita Seamount.
 1100 Some syn-sedimentary faults were active during deposition of MS3 and M4 only. A part of
 1101 these fault was reactivated later during deposition of MS5 (Anguillita Spur) and others are
 1102 recent (Saba bank).

1103

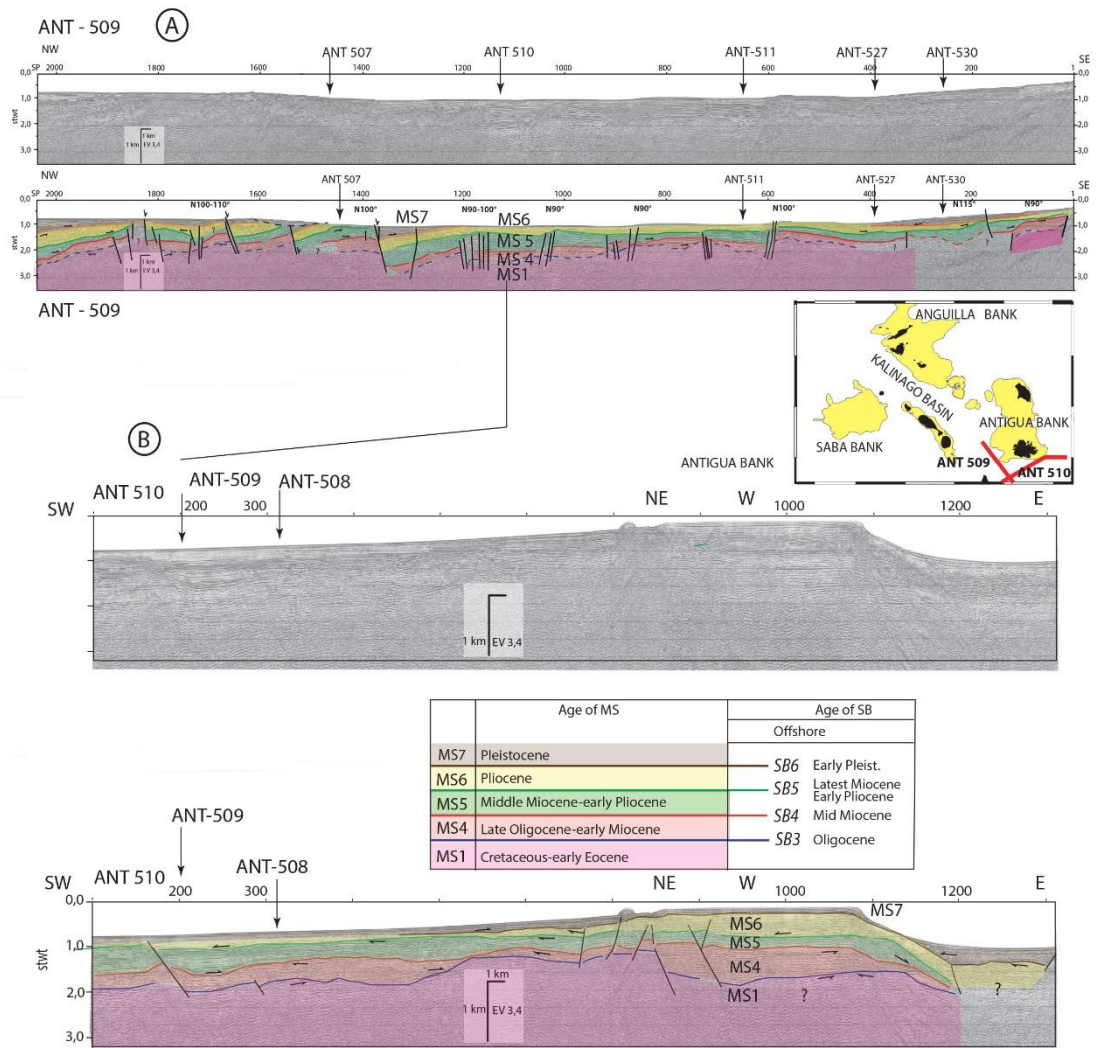


Cornée et al. Fig. 12

1104

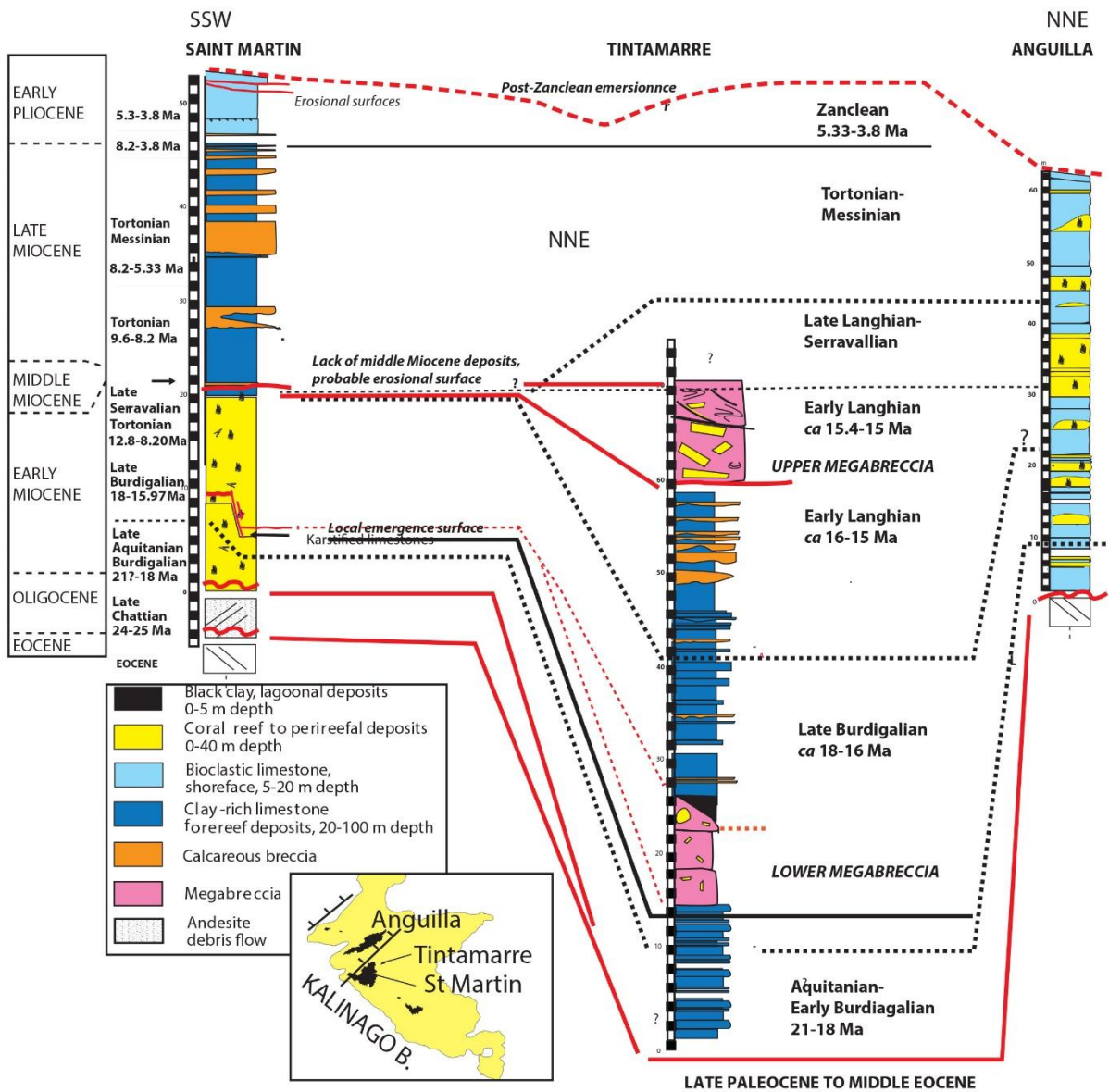
1105 Fig. 12: CPEM seismic line 302. Sequence boundaries display an erosional character. MS2 is
 1106 preserved as a relict patch only to the SE of the seismic profile below SB2. The Kalinago Rift
 1107 opened from MS3 to MS6.

1108



1109 Cornée al., Fig. 14

1110 Fig. 13: A: CPEM line 509; B: CPEM line 510. In the southern part of the Kalinago Basin,
 1111 MS2 and MS3 are missing. MS7 can be separated from MS6. The basin opened during
 1112 deposition of MS4 (late Oligocene), later than its northern part (MS3, early Oligocene).



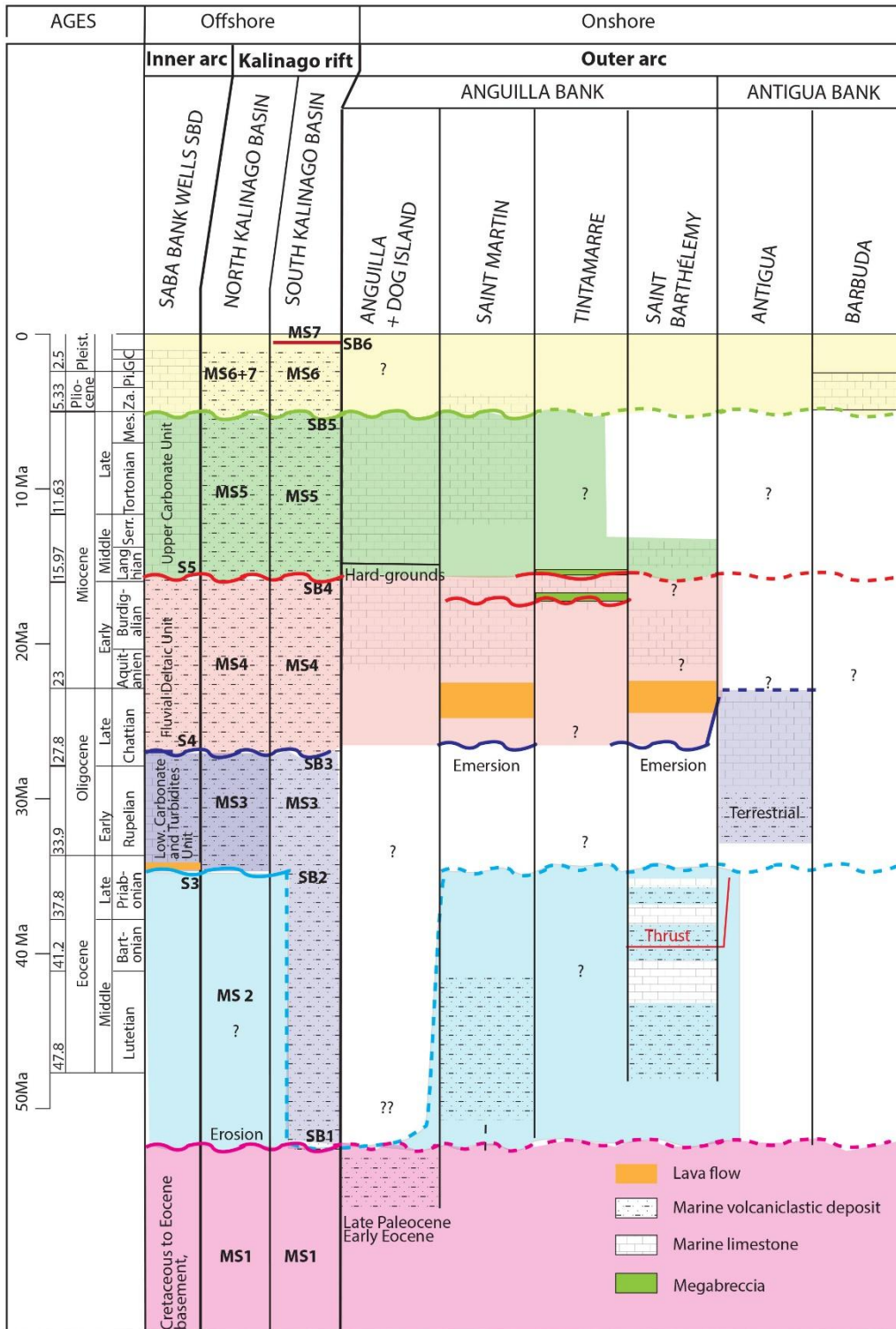
1113

Cornée et al., Fig. 14

1114 Fig. 14: Synthetic Cenozoic lithostratigraphies and correlations of St Martin, Tintamarre and
 1115 Anguilla islands.

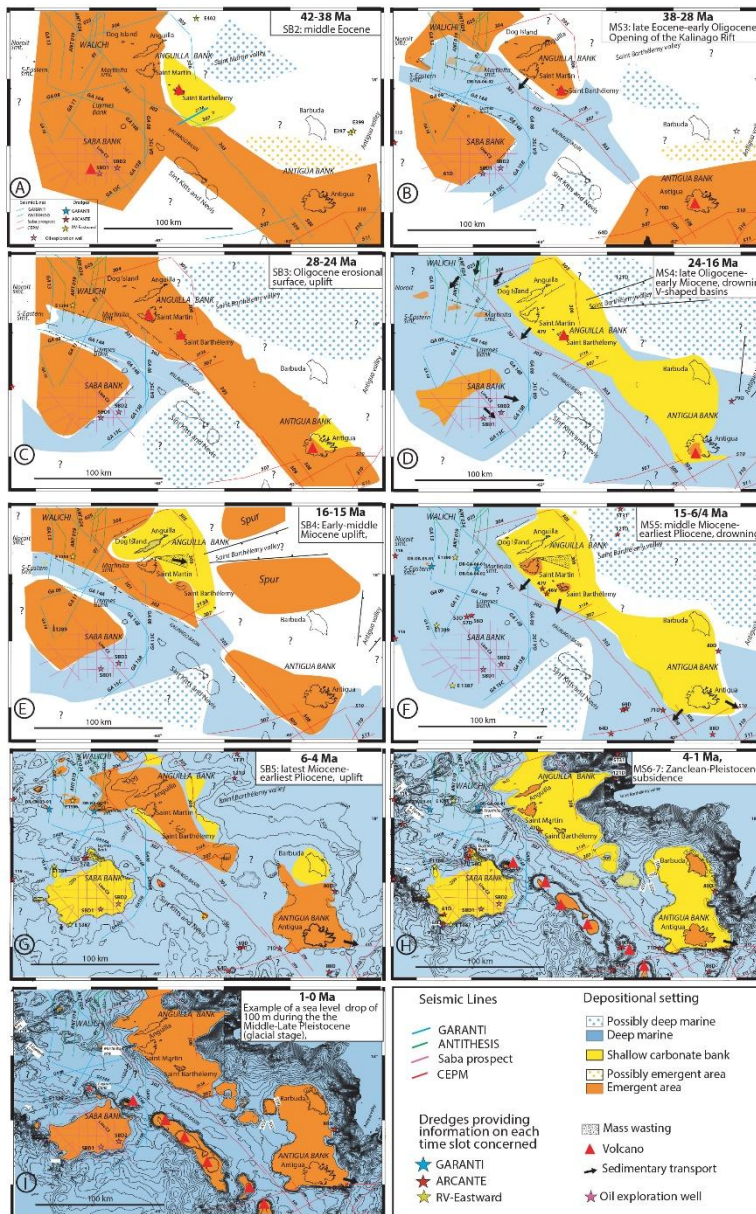
1116

1117



1118 Cornée et al., Fig. 15

1119 15: Onshore-offshore correlations in the northern Lesser Antilles. Onshore, SB2 and SB3 are
 1120 often stacked in a single erosional surfac



1121

Comde et al., Fig. 16

1122 Fig. 16: Paleogeographic maps of the northern Lesser Antilles, reconstructed from the late
 1123 Eocene to the Middle-Late Pleistocene. A: end of late Eocene compression; B:
 1124 opening of the Kalinago Basin; C: propagation of the Kalinago Basin; D: late
 1125 Oligocene-early Miocene drowning; E: opening of the V-shaped basins and uplift
 1126 (Boucard et al., 2021); F: middle Miocene-earliest Pliocene drowning; G: latest
 1127 Miocene-earliest Pliocene uplift; H: Zanclean-Calabrian drowning; I: example of
 1128 emerged areas during middle-late Pleistocene glacial maxima (considering 100 m sea
 1129 level drops). **Supplementary data**

1130

1131 Appendix A: Microphotographs of stratigraphically significant calcareous nannofossil taxa
1132 from the samples collected in the northern Lesser Antilles. Appendix B: Microphotographs of
1133 stratigraphically significant foraminiferal taxa from the samples collected in the northern
1134 Lesser Antilles.

1135

1136 Appendix C: Lithostratigraphical successions of Anguilla with depositional settings and
1137 microfossil content.

1138

1139 Appendix D: Lithostratigraphical successions of St Martin with depositional settings and
1140 microfossil content.

1141

1142 Appendix E: Lithostratigraphical successions of Tintamarre with depositional settings and
1143 microfossil content.

1144

1145 Appendix F: Lithostratigraphical succession of the Highland Fm. of Barbuda with
1146 depositional settings and microfossil content.

1147

1148 Appendix G: Lithostratigraphical successions of St Barthélemy and Antigua with depositional
1149 settings and microfossil content.

1150

1151 Appendix H: Dredged samples in the northern Lesser Antilles; locations Fig. 2.

1152

1153 Appendix I: Samples dredged during the cruise GARANTI: facies, depositional settings and
1154 microfossil contents.

1155
1156 Appendix J: Seismic lines CPEM 213 (Bouysse et al., 1994, re-interpreted) and GARANTI
1157 GA08 and 09.

1158
1159 Appendix K: Radiometric dating of a lava in St Martin, Terres Basses.

1160

1161 **References**

1162 Ali JR., 2012 Colonizing the Caribbean: is the GAARLandia land-bridge hypothesis gaining a
1163 foothold? *J. Biogeogr.* 39, 431–433. [doi:10.1111/j.1365-2699.2011.02674.x](https://doi.org/10.1111/j.1365-2699.2011.02674.x)

1164
1165
1166 Andréieff P., Bouysse P. and Westercamp D., 1980. Reconnaissance géologique de l'arc
1167 insulaire des Petites Antilles. Résultats d'une campagne à la mer de prélèvements de roches
1168 entre Sainte Lucie et Anguilla. Rapport Bur. Géol. Min., Orléans (F), 80 SGN 086 MAR, 70
1169 pp.

1170
1171 Andréieff P., Bouysse P. and Westercamp D., 1987. Géologie de l'arc insulaire des Petites
1172 Antilles, et évolution géodynamique de l'ESTCaraiibe, Thèse de Doctorat d'état, Université de
1173 Bordeaux I.

1174
1175 Andréieff P., Baubron J.C. and Westercamp D., 1988a. Histoire géologique de la Martinique
1176 (Petites Antilles): biostratigraphie (foraminifères), radiochronologie (potassium–argon),
1177 évolution volcano-structurale. *Géol. Fr.*, 2-3, 39-70.

1178
1179 Andréieff P., Westercamp D., Garrabé F. and Bonneton J.R., 1988b. Stratigraphie de l'île de
1180 Saint-Martin. *Géol. Fr.*, 2-3, 71-88.

1181
1182 Boschman L. M., van Hinsbergen D. J. J., Torsvik T. H., Spakman, W. and Pindell, J. L.,
1183 2014. Kinematic reconstruction of the Caribbean region since the Early Jurassic. *Earth-Sci.*
1184 *Rev.*, 138, 102-136.

1185
1186 Boucard M., Lebrun J.-F., Marcaillou B., Laurencin M., Klingelhoefer, F., Laigle, M.,
1187 Lallemand, S., Schenini L., Graindorge D., Cornée J.-J., Münch, P., Philippon M., and the
1188 ANTITHESIS 1, 3 Teams, 2021 (in press). Paleogene V-shaped basins and Neogene
1189 subsidence of the Northern Lesser Antilles forearc. *Tectonics*.

1190 <https://doi.org/10.1029/2020TC006524>

1191
1192 Boudagher-Fadel M. K., 2008. Evolution and significance of larger benthic foraminifera. In :
1193 Developments in Paleontology and stratigraphy 21 (ed. P. B. Wignall), 540 pp., Amsterdam,
1194 Elsevier.

1195
1196 Boudagher-Fadel M. K., 2015. Biostratigraphic and Geological Significance of Planktonic
1197 Foraminifera (Updated 2nd Edition). London, UCL Press, 298 pp.
1198 [doi:10.14324/111.9781910634257](https://doi.org/10.14324/111.9781910634257)

1199
1200 Boudagher-Fadel M.K., 2018. Revised Diagnostic First and Last Occurrences of Mesozoic
1201 and Cenozoic Planktonic Foraminifera. UCL Office of the Vice-Provost Research,
1202 Professional Papers Series, 2, 1-5. <http://www.es.ucl.ac.uk/people/fadel/home-mkf.htm>
1203
1204 Bouysse P. and Guennoc P., 1983. Données sur la structure de l'arc insulaire des Petites
1205 Antilles entre St Lucie et Anguilla. *Mar. Geol.* 53, 131– 166.
1206
1207 Bouysse P. and Mascle A., 1994. Sedimentary Basins and Petroleum Plays Around the French
1208 Antilles. In: Mascle A. (eds) Hydrocarbon and Petroleum Geology of France. Special
1209 Publication of the European Association of Petroleum Geoscientists, 4. Springer.
1210 https://doi.org/10.1007/978-3-642-78849-9_3
1211
1212 Bouysse P., Andréïeff P., Richard M., Baudron J.C., Mascle A., Maury R. and Westercamp,
1213 D., 1985a. Aves swell and northern Lesser Antilles Ridge: Rock-dredging results from
1214 ARCANTE 3 cruise. In: A. Mascle (Ed.), Caribbean geodynamics, Technip, Paris 65-76.
1215
1216 Bouysse P., Baudron J.C., Richard M., Maury R. and Andréïeff P., 1985b. Evolution de la
1217 terminaison nord de l'arc interne des Petites Antilles au Plio-Quaternaire. *Bull.Soc.géol. Fr.*, I,
1218 181–188. <https://doi.org/10.2113/gssgfbull.1.2.181>
1219
1220 Brace S., Turvey S. T., Weksler M., Hoogland M. L. P. and Barnes I., 2015. Unexpected
1221 evolutionary diversity in a recently extinct Caribbean mammal radiation. *Proc. Roy.Soc.*
1222 *London*, B, 282, 20142371.
1223
1224 Brasier M. D. and Mather J.D., 1975. The stratigraphy of Barbuda, West Indies. *Geol. Mag.*,
1225 112, 271-282.
1226
1227 Brasier M.D. and Donahue J., 1985. Barbuda-An emerging reef and lagoon complex on the
1228 edge of the Lesser Antilles island arc. *J. geol. Soc. London*, 142, 1101-1117.
1229
1230 Briden J. C., Rex D. C., Faller A. M. and Tomblin J. F., 1979. K-Ar geochronology and
1231 palaeomagnetism of volcanic rocks in the Lesser Antilles island arc. *Philos. Trans. Royal Soc.*
1232 *A: Mathematical, Physical and Engineering Sciences*, 291, 485–528.
1233 doi.org/10.1098/rsta.1979.0040
1234
1235 Budd A.F., Johnson K.G. and Edwards J.C., 2005. Caribbean reef coral diversity during the
1236 early to middle Miocene: an example from the Anguilla Formation. *Coral reefs*, 14, 109-117.
1237
1238 Calais E., Symithe S., de Lépinay B. M. and Prépetit C., 2016. Plate boundary segmentation
1239 in the northeastern Caribbean from geodetic measurements and Neogene geological
1240 observations. *C. R. Geoscience*, 348, 42-51.
1241
1242 Carey S., Sparks R. S. J., Tucker M. E., Li T., Robinson L., Watt S. F. L., ... and Ballard R.
1243 D., 2020. The polygenetic Kahouanne Seamounts in the northern Lesser Antilles island arc:
1244 evidence for large-scale volcanic island subsidence. *Marine Geology*, 419,
1245 <https://doi.org/10.1016/j.margeo.2019.106046>.
1246
1247 Cattuneanu O., 2006. Principles of sequence stratigraphy. Elsevier, 369 pp.
1248

1249 Chaytor J. D. and ten Brink U. S., 2015. Event sedimentation in low-latitude deep-water
1250 carbonate basins, Anegada Passage, northeast Caribbean. *Basin Res.*, 27, 310–335.
1251 [doi:10.1111/bre.12076](https://doi.org/10.1111/bre.12076).
1252

1253 Christman R. A., 1953. Geology of St Bartholomew, St Martin, and Anguilla, Lesser Antilles.
1254 *Geol. Soc. Amer., Bull.*, 64, 65–96. [https://doi.org/10.1130/0016-
1255 7606\(1953\)64%5B85:GOSBSM%5D2.0.CO;2](https://doi.org/10.1130/0016-7606(1953)64%5B85:GOSBSM%5D2.0.CO;2)
1256

1257 Church R. E. and Allison K. R., 2004. The Petroleum Potential of the Saba Bank Area, Netherlands
1258 Antilles. Search and
1259 Discovery Article # 10076. Posted December 20, 2004

1260 Clark, S.A., Sobiesiak, M., Zelt, C.A., Magnani, M.B., Miller, M.S., Bezada, M.J.,
1261 Levander, A., 2008. Identification and tectonic implications of a tear in the South American
1262 plate at the southern end of the Lesser Antilles. *Geochemistry, Geophysics, Geosystems*, 9,
1263 Q11004. [doi:10.1029/2008GC002084](https://doi.org/10.1029/2008GC002084).
1264

1265 Cornée J.-J., Léticée J.-L., Münch P., Quillévéré F., Lebrun J.-F., Moissette P., Braga J.C.,
1266 Melinte- Dobrinescu M., De Min L., Oudet J., Randrianasolo A., 2012. Sedimentology,
1267 paleoenvironments and biostratigraphy of the Pliocene- Pleistocene carbonate platform of
1268 Grande- Terre (Guadeloupe, lesser Antilles fore-arc). *Sedimentology*, 59, 1426- 1451.
1269

1270 Cornée J.- J., BouDagher- Fadel M., Philippon M., Léticée J.- L., Legendre L., Maincent G.,
1271 Lebrun J.- F., and Münch P., 2020 Paleogene carbonate systems of Saint Barthélemy, Lesser
1272 Antilles: stratigraphy and general organisation. *Newsl. Stratigr.* [doi:10.1127/nos/2020/0587](https://doi.org/10.1127/nos/2020/0587).
1273

1274 Courcelle M., Tilak M.-K., Leite Y. L. R., Douzery E. J. P. and Fabre, P.-H., 2019. Digging
1275 for the spiny rat and hutia phylogeny using a gene capture approach, with the description of a
1276 new mammal subfamily. *Mol. Phylog. Evol.*, 136, 241-253.
1277

1278 Coussens M.F. *et al.*, 2012. Synthesis: stratigraphy and age control for IODP Sites U1394,
1279 U1395, and U1396 offshore Montserrat in the Lesser Antilles. *In: Le Friant, A., Ishizuka, O.,*
1280 *Stroncik, N.A., and the Expedition 340 Scientists. Proc. IODP 340.*
1281 [doi:10.2204/iodp.proc.340.204.2016](https://doi.org/10.2204/iodp.proc.340.204.2016).
1282

1283 Dagain J., Andréieff P., Westercamp D., Bouysse P. and Garrabé F., 1989. Carte géologique
1284 de France (1:50000), feuille Saint Martin. Bureau de Recherches Géologiques et Minières,
1285 Orléans (Fr).
1286

1287 Dávalos L. M., 2004. Phylogeny and biogeography of Caribbean mammals. *Biol. J. Linnean*
1288 *Soc.*, 81, 373-394.
1289

1290 Dailey S.K., Clift P.D., Kulhanek D.K *et al.*, 2019. Large-scale mass wasting on the Miocene
1291 continental margin of western India. *Geol. Soc. Amer. Bull.*, 132, 85-112.
1292 doi.org/10.1130/B35158.1
1293

1294 Daly T.E. (1995) The Petroleum Potential of the Netherlands Antilles. *In: Miller R.L.,*
1295 *Escalante G., Reinemund J.A., Bergin M.J. (eds), Energy and Mineral Potential of the Central*
1296 *American-Caribbean Region. Circum-Pacific Council for Energy and Mineral Resources*
1297 *Earth Science Series*, 16, Springer. https://doi.org/10.1007/978-3-642-79476-6_14

1298 Defand M.J., Sherman S., Maury R.C., Bellon H. de Boer J., Davidson J. and Kepezhinskas
1299 P., 2001. The geology, petrology, and petrogenesis of Saba Island, Lesser Antilles. *J. Volc.*
1300 *Geoth. Res.*, 107, 87-111.
1301
1302 Delsuc F., Kuch M., Gibb G. C., Karpinski E., Hackenberger D., Szpak P., Martinez J. G.,
1303 Mead J. I., McDonald H. G., MacPhee R. D. E. Billet, G., Hautier L. and Poinar H. N., 2019.
1304 Ancient mitogenomes reveal the evolutionary history and biogeography of sloths. *Current*
1305 *Biology*, 29, 1-12.
1306
1307 De Min L., 2014. Sismo-stratigraphie multi-échelle d'un bassin avant-arc: Architecture du
1308 bassin de Marie-Galante, Petites Antilles. Sciences de la Terre. *PhD Thesis*, Université des
1309 Antilles et de la Guyane (UAG), Pointe à Pitre, Guadeloupe, F. [https://hal.archives-](https://hal.archives-ouvertes.fr/tel-03144281)
1310 [ouvertes.fr/tel-03144281](https://hal.archives-ouvertes.fr/tel-03144281)
1311 De Min L., Lebrun J. F., Cornée J. J., Münch P., Léticée J. L., Quillévére, F., et al., 2015.
1312 Tectonic and sedimentary architecture of the Karukéra spur: A record of the Lesser Antilles
1313 fore-arc deformations since the Neogene. *Marine Geology*, 363, 15–37.
1314 <https://doi.org/10.1016/j.margeo.2015.02.007>
1315
1316 Donovan S. K., Jackson T. A., Harper D. A., Portell, R. W. and Renema W., 2014. The upper
1317 Oligocene of Antigua: the volcanic to limestone transition in a limestone Caribbee. *Geology*
1318 *Today*, 30, 151-158.
1319
1320 Fabre P.-H., Vilstrup J. T., Raghavan M., Der Sarkissian C., Willerslev E., Douzery E. J. P.
1321 and Orlando, L., 2014. Rodents of the Caribbean: origin and diversification of hutias
1322 unravelled by next-generation museomics. *Biol. Lett.*, 10, 20140266.
1323
1324 Favier A., Lardeaux J.-M., Legendre L., Verati C., Philippon M., Corsini M., Münch P. and
1325 Ventalon S., 2019. Tectono-metamorphic evolution of shallow crustal levels within active
1326 volcanic arcs. Insights from the exhumed Basal Complex of Basse-Terre (Guadeloupe, French
1327 West Indies). *BSGF - Earth Sci. Bull.*, 190, 10. <https://doi.org/10.1051/bsgf/2019011>
1328
1329 Feuillet, N., Manighetti, I., Tapponnier, P., Jacques, E., 2002. Arc parallel extension and
1330 localization of volcanic complexes in Guadeloupe, Lesser Antilles. *J. Geophys. Res.: Solid*
1331 *Earth*, 107 ETG 3-1–ETG 3-29.
1332
1333 Feuillet N., Leclerc F., Tapponnier P., Beauducel F., Boudon G., Le Friant A., Deplus C.,
1334 Lebrun J.-F., Nercessian A., Saurel J.-M. and Clément V., 2010. Active faulting induced by
1335 slip partitioning in Montserrat and link with volcanic activity: New insights from the 2009
1336 GWADASEIS marine cruise data. *Geoph. Res. Letters*, 37, L00E15. [doi:10.1029/2010GL042556](https://doi.org/10.1029/2010GL042556),
1337
1338 Feuillet N., Beauducel F. and Tapponnier P., 2011. Tectonic context of moderate to large
1339 historical earthquakes in the Lesser Antilles and mechanical coupling with volcanoes. *J.*
1340 *Geophys. Res.: Solid Earth* 116(B10).
1341
1342 Fox P. J., Schreiber E. and Heezen B. C., 1971. The geology of the Caribbean crust: Tertiary
1343 sediments, granitic and basic rocks from the Aves Ridge. *Tectonophysics*, 12, 89–109.
1344

1345 Frost S.H. and Weiss M.P., 1979. Patch reef communities and succession in the Oligocene of
1346 Antigua, West Indies. *Geol. Soc. Amer. Bull.*, 90, 1094-1141.
1347

1348 Garrocq C., Lallemand S., Marcaillou B., Lebrun J.-F., Padron C., Klingelhofer F., Laigle
1349 M., Munch P., Gay A., Shenini L., Beslier M.-O., Cornée J.-J., Mercier De Lepinay B.,
1350 Quillevère F. and Boudagher-Fadel M., 2020. Genetic relations between the Aves Ridge and
1351 the Grenada back-arc basin, East Caribbean Sea. *J. Geophys. Res. Solid Earth*, 126,
1352 e2020JB020466. <https://doi.org/10.1029/2020JB020466>
1353

1354 Gomez S., Bird D. and Mann P., 2018. Deep crustal structure and tectonic origin of the
1355 Tobago-Barbados ridge. *Interpretation*, 6 (2): T471–T484. [https://doi.org/10.1190/INT-2016-](https://doi.org/10.1190/INT-2016-0176.1)
1356 [0176.1](https://doi.org/10.1190/INT-2016-0176.1)
1357

1358 Gradstein F. M., Ogg J. G., Schmitz M. D., Ogg G. M., 2012. The Geologic Time Scale 2012.
1359 Elsevier, 1- 144.

1360 Hastie A.R., Cox S. and Kerr A.C., 2021. Northeast- or southwest-dipping subduction in the
1361 Cretaceous Caribbean gateway? *Lithos*. <https://doi.org/10.1016/j.lithos.2021.105998>
1362

1363 Hedges S. B., 1996. Historical biogeography of West Indian vertebrates. *Ann. Rev. Ecol.*
1364 *System.*, 27, 163-196.
1365

1366 Hedges S.B., 2001. Caribbean biogeography: an outline. In: Biogeography of the West Indies:
1367 patterns and perspectives (eds CA Woods, FE Sergile), CRC Press, Boca Raton, FL ,15–33.
1368

1369 Hedges S.B., 2006. Palaeogeography of the Antilles and origin of the West Indian terrestrial
1370 vertebrates. *Annals of the Missouri Botanical Garden*, 93, 231-244.
1371

1372 Hedges S.B., Hass C.A., Maxson L.R., 1992. Caribbean biogeography: molecular evidence
1373 for dispersal in West Indian terrestrial vertebrates. *Proc. Natl Acad. Sci. USA*, 89, 1909–1913.
1374 doi:10.1073/pnas.89.5.1909
1375

1376 Hine A.C., Locker S.D., Tedesco L.P., Mullins H.T., Hallock P., Belknap D.F., Gonzales J.L.,
1377 Neuman A.C. and Snyder S.W, 1992. Megabreccia shedding from modern, low-relief
1378 carbonate platforms, Nicaraguan Rise. *Geol. Soc. Amer. Bull.*, 104, 928-943.
1379

1380 Iturralde-Vinent M. A., 2006. Meso-Cenozoic Caribbean palaeogeography: implications for
1381 the historical biogeography of the region. *Int. Geol. Rev.*, 48, 791-827.
1382

1383 Iturralde- Vinent M.A. and MacPhee R.D.E., 1999 Palaeogeography of the Caribbean region:
1384 implications for Cenozoic biogeography. *Bull. Am. Mus. Nat. Hist*, 238, 1–95.
1385

1386 Jany I., 1989. Néotectonique au sud des Grandes Antilles: Collision (ride de Beata, presqu’île
1387 de Bahoruco): Subduction (fosse de Los Muertos), transtension (passage d’Anegada). PhD
1388 Thesis, University Pierre et Marie Curie, 300 p.
1389

1390 Jany I., Scanlon K. M. and Mauffret, A., 1990. Geological interpretation of combined
1391 Seabeam, Gloria and seismic data from Anegada Passage (Virgin Islands, north Caribbean).
1392 *Mar. Geophys. Res.* 12, 173-196. <https://doi.org/10.1007/BF02266712>
1393

1394 Jolly W.T., Lidiak E.G., Schellekens J.H. and Santos, H., 1998. Volcanism, tectonics, and
1395 stratigraphic correlations in Puerto Rico. *Geol. Soc. Am. Spec. Pap.*, 322, 1–34.
1396

1397 Land L.S., MacKenzi F.E. and Gould S.J., 1967. Pleistocene history of Bermuda. *Geol. Soc.*
1398 *Amer. Bull.*, 78, 993-1106.
1399

1400 Larue D.K. and Warner A.J. 1991. Sedimentary basins of the NE Caribbean Plate boundary
1401 zone and their petroleum potential. *J. Petr. Geol.*, 14. [https://doi.org/10.1111/j.1747-](https://doi.org/10.1111/j.1747-5457.1991.tb00312.x)
1402 [5457.1991.tb00312.x](https://doi.org/10.1111/j.1747-5457.1991.tb00312.x)
1403

1404 Laurencin M., Marcaillou B., Graindorge D., Klingelhofer F., Lallemand S., Laigle M. and
1405 Lebrun J.-F., 2017. The polyphased tectonic evolution of the Anegada Passage in the northern
1406 Lesser Antilles subduction zone. *Tectonics*, 36, 945–961.
1407 <https://doi.org/10.1002/2017TC004511>
1408

1409 Laurencin M., Graindorge D., Klingelhofer F., Marcaillou B. and Evain M., 2018.
1410 Influence of increasing convergence obliquity and shallow slab geometry onto tectonic
1411 deformation and seismogenic behavior along the Northern Lesser Antilles zone. *Earth Planet.*
1412 *Sci. Lett.*, 492, 59-72
1413

1414 Lebrun J.F. and Lallemand S., 2017. Unpublished GARANTI cruise report.
1415 <http://dx.doi.org/10.17600/17001200>
1416

1417 Legendre L., 2018. Cinématique des déformations fragiles dans la partie Nord de l’arc des
1418 Petites Antilles. PhD Thesis, Université des Antilles.
1419

1420 Legendre L., Philippon M., Münch P., Leticée J. L., Noury M., Maincent, G., Cornée J.-J.,
1421 2018. Trench bending initiation: Upper plate strain pattern and volcanism. Insights from the
1422 Lesser Antilles arc, St Barthelemy Island, French West Indies. *Tectonics*, 37, 2777–2797.
1423 <https://doi.org/10.1029/2017TC004921>
1424

1425 Mac Donald R., Hawkesworth C. J. and Heath E., 2000. The Lesser Antilles volcanic chain:
1426 A study in arc magmatism. *Earth Sci. Rev.*, 49, 1–76.
1427

1428 MacPhee R. D. E., 2005. 'First' appearances in the Cenozoic land-mammal record of the
1429 Greater Antilles: significance and comparison with South American and Antarctic records. *J.*
1430 *Biogeogr.*, 32, 551-564.
1431

1432 MacPhee R.D.E. and Iturralde- Vinent M.A., 1995. Origin of the Greater Antillean land
1433 mammal fauna, 1: New Tertiary fossils from Cuba and Puerto Rico. *Am. Mus. Novit.* 3141, 1-
1434 30.
1435

1436 Mann P., Taylor F.W., Lawrence Edwards R. and Ku T., 1995. Actively evolving microplate
1437 formation by oblique collision and sideways motion along strike-slip faults: An example from
1438 the northeastern Caribbean plate margin. *Tectonophysics*, 246, 1-69.
1439

1440 Mann P., Hippolyte J.C., Grindlay N.R. and Abrams L.J., 2005. Neotectonics of southern
1441 Puerto Rico and its offshore margin, in: Mann, P. (Ed.), Active tectonics and seismic hazards
1442 of Puerto Rico, the Virgin Islands and off-shore areas. *Geol. Soc. Am. Spec. Paper*, 385, 115-
1443 138.
1444

1445 Marcaillou B. and Klingelhoefer F., 2013. ANTITHESIS-1-Leg1 Cruise, RV L'Atalante,
1446 doi:10.17600/13010070.
1447
1448 Marcaillou, B., Klingelhoefer, F., 2016. ANTITHESIS-3 Cruise, RV Pourquoi Pas?,
1449 doi:10.17600/16001700
1450
1451 Marivaux L., Vélez-Juarbe J., Merzeraud G., Pujos F., Viñola López L. W., Boivin M.,
1452 Santos-Mercado H., Cruz E. J., Grajales A., Padilla J., Vélez-Rosado K. I., Philippon M.,
1453 Léticée J.-L., Münch P. and Antoine P.-O., 2020. Early Oligocene chinchilloid caviomorphs
1454 from Puerto Rico and the initial rodent colonization of the West Indies. *Proc. Roy. Soc. B*,
1455 287, 20192806.
1456
1457 Martin-Kaye P.H.A., 1969. A summary of the geology of the Lesser Antilles. *Overseas Geol.*
1458 *Miner. Resour.*, 10, 172-206.
1459
1460 Mascle A. and Westercamp D., 1983. Géologie d'Antigua, Petites Antilles. *Bull. Soc. Géol.*
1461 *Fr.*, 7, 855-866.
1462
1463 Matchette-Downes C., 2007. Saba Bank, Dutch Antilles petroleum potential. Saba Bank
1464 Petroleum Resources, 19 pp. <https://www.mdoil.co.uk/pdfs/Curacao.pdf>
1465
1466 Mauffret A. and Jany I., 1990. Collision et tectonique d'expulsion le long de la frontière Nord-
1467 Caraïbe. *Oceanologica Acta*, spec. vol. 10, 97-116.
1468
1469 McCann W.R. and Sykes L.R., 1984. Subduction of aseismic ridges beneath the Caribbean
1470 Plate: Implications for the tectonics and seismic potential of the northeastern Caribbean. *J.*
1471 *Geophys. Res.* 89, 4493-4519, [doi:10.1029/JB089iB06p04493](https://doi.org/10.1029/JB089iB06p04493).
1472
1473 Mittermeier R. A., Turner W. R., Larse, F. W., Brooks T. M. and Gascon, C., 2011. Global
1474 Biodiversity Conservation: The Critical Role of
1475 Hotspots in Biodiversity Hotspots. Springer (eds Zachos F. E. and Habel J. C.), 3-22.
1476
1477 Montaggioni L. and Braithwaite C.J.R., 2009. Structure, zonation and dynamic patterns of
1478 coral reef communities. *Developments in Marine Geology*, 5, 67-122, Elsevier. [doi:](https://doi.org/10.1016/S1572-5480(09)05003-9)
1479 [10.1016/S1572-5480\(09\)05003-9](https://doi.org/10.1016/S1572-5480(09)05003-9)
1480
1481 Multer H.G., Weiss M.P. and Nicholson D.V., 1986. Antigua; reefs, rocks and highroads of
1482 history. Leeward Island Science Associates, St John's, Antigua, Contrib. 1, 116 pp.
1483
1484 Münch P., Lebrun J.-F., Cornée J.-J., Thinon I., Guennoc P., Marcaillou B., Randrianasolo A.
1485 and the KASHALLOW TEAM, 2013. Pliocene to Pleistocene carbonate systems of the
1486 Guadeloupe archipelago, French Lesser Antilles: a land and sea study. *Bulletin de la Société*
1487 *géologique de France*, 184, 99-110.
1488
1489 Münch, P., Cornée, J.-J., Lebrun, J.F., Quillévéré, F., Vérati, C., Melinte-Dobrinescu, M.,
1490 Demory, F., Smith, M.J., Jourdan, X., Lardeaux, J.-M., De Min L., Léticée J.-L. and
1491 Randrianasolo A., 2014. Pliocene to Pleistocene vertical movements in the forearc of the
1492 Lesser Antilles subduction: insights from chronostratigraphy of shallow-water carbonate
1493 platforms (Guadeloupe archipelago). *J. Geol. Soc. London*, 171, 329-341.
1494

- 1495 Myers N., Russell A., Mittermeier R.A., Mittermeier C.G., da Fonseca G.A.B. and Kent J.,
 1496 2000. Biodiversity hotspots for conservation priorities. *Nature*, 403, 853-858.
 1497
- 1498 Nagle F., Stipp J. J. and Fisher D. E., 1976. K-Ar geochronology of the limestone caribbees
 1499 and Martinique, Lesser Antilles, West Indies. *Earth Planet. Sci. Lett.*, 29, 401–412.
 1500
- 1501 Nairn A. and Stehli F.G. eds., 1975. Geology of the Caribbean crust, Gulf of Mexico and the
 1502 Caribbean. Plenum press, 1975.
 1503
- 1504 Neill I., Kerr A. C., Hastie A. R., Stanek K. P. and Millar I. L., 2011. Origin of the Aves Ridge
 1505 and Dutch–Venezuelan Antilles: Interaction of the Cretaceous ‘Great Arc’ and Caribbean–
 1506 Colombian Oceanic Plateau? *J. Geol. Soc. London*, 168, 333–348.
- 1507 Padron C., Klingelhoefer F. Marcaillou B., Lebrun J.-F., Lallemand S., Garrocq C., Laigle
 1508 M., Roest W. R., Schenini L., Beslier M.-O., Graindorge D., Gay A., Audemard F., Münch Ph.
 1509 and the GARANTI Cruise Team, 2020. Deep Structure of the Grenada Basin From
 1510 Wide- Angle Seismic, Bathymetric and Gravity Data. *J. Geoph. Res.*, 126, e2020JB020472.
 1511 <https://doi.org/10.1029/2020JB020466>
- 1512 Philippon M. and Corti G., 2016. Obliquity along plate boundaries. *Tectonophysics*, 693, 171-
 1513 182. <https://doi.org/10.1016/j.tecto.2016.05.033>
 1514
- 1515 Philippon M., Cornée J.-J., Münch P., van Hinsbergen D.J.J., BouDagher-Fadel M., Gailler
 1516 L., Quillévéré F., Boschman L., Montheil L., Gay A., Lebrun J.-F., Lallemand S., Marivaux
 1517 L. and Antoine P.O., 2020a. Eocene intra-plate shortening responsible for the rise of a fauna
 1518 pathway in the northeastern Caribbean realm. *Plos-ONE*, 15(10): e0241000.
 1519 <https://doi.org/10.1371/journal.pone.0241000>
 1520
- 1521 Philippon M., Boschman L.M., Gossink L.A.W., Munch P., Cornée J.-J., Boudagher-Fadel
 1522 M., Léticée J.L., Lebrun J.-F. and Van Hinsbergen D.J.J., 2020b. Paleomagnetic evidence
 1523 from St. Barthélemy Island for post-Eocene rotation and deformation in the forearc of the
 1524 curved Lesser Antilles subduction zone. *Tectonophysics*, 777, 228323.
 1525 <https://doi.org/10.1016/j.tecto.2020.228323>
 1526
- 1527 Pindell J. L. and Kennan L., 2009. Tectonic evolution of the Gulf of Mexico, Caribbean and
 1528 northern South America in the mantle reference frame: an update. Geological Society,
 1529 London, Special Publications 328, 1-55, [doi:10.1144/SP328.1](https://doi.org/10.1144/SP328.1).
 1530
- 1531 Presslee S., Slater, G. J., Pujos F., Forasiepi A. M., Fischer R., Molloy K., Mackie M., Olsen
 1532 J. V., Kramarz A. G., Taglioretti M., Scaglia F., Lezcano M., Lanata J. L., Southon J., Feranec
 1533 R., Bloch J. I., Hajduk A., Martin F. M., Salas-Gismondi R., Reguero M. A., de Muizon C.,
 1534 Greenwood A., Chait B. T., Penkman K., Collins M. and MacPhee R. D. E., 2019.
 1535 Palaeoproteomics resolves sloth relationships. *Nat. Ecol. Evol.*, 3, 1121–1130.
 1536
- 1537 Railsback L.B., Gibbard P.L., Head M.J., Voarintsoa N.R.G. and Toucanne S., 2015. An
 1538 optimized scheme of lettered marine isotope substages for the last 1.0 million years, and the
 1539 climatostratigraphic nature of isotope stages and substages. *Quat. Sci. Rev.*, 111, 94–106.
 1540 Rankin D.W., 2002. Geology of St John, U.S. Virgin Islands. U.S. Geol. Surv. Prof. Paper
 1541 1631, 36 pp.
 1542
- 1543 Reed F.R.C., 1921. The Geology of the British Empire. Edward Arnold, London.

1544 Robinson E. D., Paytan A. D. and Chien C. T., 2017. Strontium isotope dates for the
1545 Oligocene Antigua Formation, Antigua, WI. *Caribb. J. Earth Sci.*, 50, 11-18.
1546

1547 Roca A. L., Bar-Gal G., Eizirik E., Helgen K. M., Maria R., Springer M. S., O'Brien, S. J. and
1548 Murphy W. J., 2004. Mesozoic origin for West Indian insectivores. *Nature*, 429, 649-651.
1549

1550 Roksandic M.M., 1978. Seismic facies analysis concepts. *Geophys. Prospect.*, 26, 383-398.
1551 Russell R. J. and McIntire W. J. 1966. Barbuda reconnaissance. *Tech. Rep. coastal Stud. Inst*
1552 *La St Univ.*, 11 (J), 1-53.
1553

1554 Samper A, Quidelleur X, Lahitte P, Mollex D. 2007. Timing of effusive volcanism and
1555 collapse events within an oceanic arc island: Basse-Terre, Guadeloupe archipelago (Lesser
1556 Antilles Arc). *Earth Planet. Sci. Letters* 258, 175–191. [DOI: 10.1016/j.epsl.2007.03.030](https://doi.org/10.1016/j.epsl.2007.03.030).

1557 Scotese, C.R., 2016. PALEOMAP PaleoAtlas for GPlates and the PaleoData Plotter Program,
1558 PALEOMAP Project, <http://www.earthbyte.org/paleomap---paleoatlas---for---gplates>
1559

1560 Speed R. C., Gerhard L. C. and McKee E. H., 1979. Ages of deposition, deformation, and
1561 intrusion of Cretaceous rocks, eastern St Croix, Virgin Islands. *Geol. Soc. Amer. Bull.*, 90,
1562 629-632.
1563

1564 Stéphan J.F., Mercier de Lépinay B., et al., 1990. Paleogeodynamics maps of the Caribbean-
1565 14 steps from Lias to Present. *Bull. Soc. géol. Fr.* 6, 915-919.
1566

1567 Tucker M.E. and Wright, V.P., 1990. Diagenetic processes, products and environments. *In:*
1568 *Carbonate Sedimentology*. Blackwell Publishing Ltd, Oxford, U.K., 314–364.
1569

1570 Vail P. R., Mitchum R. M. and Thompson S., 1977, Seismic stratigraphy and global changes
1571 of sea level, Part 3: Relative changes of sea level from coastal onlap. *In: Seismic*
1572 *Stratigraphy—Applications to Hydrocarbon Exploration* (Ed. Payton, C. W.): American
1573 Association Geologists Memoir, 26, 83-97.
1574

1575 Van Duyle F.C. and Meesters E.H., 2018. Cruise report RV Pelagia 64PE433, Saba, St
1576 Eustatius and Saba Bank. 26 February-10 March 2018, St Maarten-St Maarten (NICO
1577 expedition leg 6). [https://www.dcbd.nl/document/cruise-report-rv-pelagia-64pe433-saba-st-](https://www.dcbd.nl/document/cruise-report-rv-pelagia-64pe433-saba-st-eustatius-and-saba-bank-benthic-habitat-mapping)
1578 [eustatius-and-saba-bank-benthic-habitat-mapping](https://www.dcbd.nl/document/cruise-report-rv-pelagia-64pe433-saba-st-eustatius-and-saba-bank-benthic-habitat-mapping) and [https://www.saba-news.com/saba-bank-has-](https://www.saba-news.com/saba-bank-has-the-deepest-and-largest-marine-sinkholes-in-the-world/)
1579 [the-deepest-and-largest-marine-sinkholes-in-the-world/](https://www.saba-news.com/saba-bank-has-the-deepest-and-largest-marine-sinkholes-in-the-world/)
1580

1581 Van Wagoner C., Posamentier H. W., M. Mitchum R., Vail P. R., Sarg J. F., Loutit T. S. and
1582 J. Hardenbol J., 1988. An overview of the fundamentals of sequence stratigraphy and key
1583 definitions. *In: Sea-Level Changes—An Integrated Approach*, SEPM Special Publication, 42,
1584 39-45
1585

1586 Wade B.S., Pearson P.N., Berggren W.A. and Paëlike H., 2011. Review and revision of
1587 Cenozoic tropical planktonic foraminiferal biostratigraphy and calibration to the geomagnetic
1588 polarity and astronomical time scale. *Earth Sci. Rev.*, 104, 111-142.
1589

1590 Warner A.J., 1990. The Cretaceous age sediments of the Saba Bank and their petroleum
1591 potential. *In: Larue DK, Draper G (eds), Trans. 12 th Caribbean Conference, St Croix. Miami*
1592 *Geol. Soc.*, South Miami, 341–354

1593
1594 Watters D., Donahue J. and Stuckenrath R., 1991. Paleoshorelines and the prehistory of
1595 Barbuda, West Indies. *In: Paleoshorelines and Prehistory: an investigation method* (Jonhson
1596 L.L. ed.). CRC Press, London, 15-51.
1597
1598 Weiss M.P., 1994. Oligocene limestones of Antigua, West Indies: Neptune succeeds
1599 Vulcan. *Caribb. J. Earth Sci.*, 30, 1-29.
1600
1601 Westercamp D., 1988. Magma generation in the Lesser Antilles: geological constraints.
1602 *Tectonophysics*, 149, 145-163. [doi: 10.1016/0040-1951\(88\)90123-0](https://doi.org/10.1016/0040-1951(88)90123-0)
1603
1604 Westercamp D., Andréieff P., Bouysse P. and Mascle A.,1985. The Grenadines, southern
1605 Lesser Antilles. Part I. Stratigraphy and volcano-structural evolution. *Carr. Geod.*
1606
1607 Woods C. A., Borroto Paéz R. and Kilpatrick C. W. 2001. Insular patterns and radiations of
1608 West Indian rodents. *In: Biogeography of the West Indies: Patterns and Perspectives* (Woods
1609 C. A. and Sergile F. E. Eds), 335-353. Boca Raton: CRC Press.
1610
1611 Wright V. P. and Burchette T. P., 1996. Shallow-water carbonate environments. *In:*
1612 *Sedimentary Environments: Processes, Facies, and Stratigraphy* (ed. H. G. Reading), 325–94.
1613 Oxford, Blackwell Science.
1614
1615 Zachariasse W.J., van Hinsbergen D.J.J. and Fortuin A.R., 1988. Mass wasting and uplift on
1616 Crete and Karpathos during the early Pliocene related to initiation of south Aegean left-
1617 lateral, strike-slip tectonics. *Geol. Soc. Amer. Bull.*, 120, 976–993. [doi: 10.1130/B26175.1](https://doi.org/10.1130/B26175.1)